R. & M. No. 3417

MINISTRY OF AVIATION

AERONAUTICAL RESEARCH COUNCIL
REPORTS AND MEMORANDA

A Theoretical Treatment of Noise and Non-Linearities in a Beam-Riding System

By E. G. C. BURT

LONDON: HER MAJESTY'S STATIONERY OFFICE
1966

PRICE 14s. 6d. NET

A Theoretical Treatment of Noise and Non-Linearities in a Beam-Riding System

By E. G. C. Burt

Reports and Memoranda No. 3417
November, 1951

Summary.

The effectiveness of a beam-riding missile is greatly influenced by the mutual effect of noise and non-linearities. The former is mostly due to radar jitter, while the principal non-linearity is that introduced by limiting the lateral acceleration of the missile to a safe value. For the beam-riding system discussed in this paper the degree of saturation is such that the linear analysis is inadequate, and account must be taken of the non-linearity. With certain assumptions, the system can be described analytically: further approximations lead to optimum values of the disposable parameters for obtaining the minimum miss distance.

The analysis shows that, while optimum values of the parameters can be specified for a restricted class of target trajectories, a more detailed study of likely target manoeuvres is necessary before an overall optimum can be defined.

LIST OF CONTENTS

Section

LIST OF APPENDICES

LIST OF TABLES

LIST OF ILLUSTRATIONS

1. *Introduction.*

1.1. The guidance accuracy of a beam-riding missile is considerably influenced by jitter of the radar beam, which gives false information to the system concerning the target motion. Since the jitter spectrum embraces the bandwidth arising from target manoeuvre, it is not possible to eliminate the jitter by filtering without losing relevant target information. In a completely linear system, the mean miss distance when attacking a manoeuvring target is not affected by jitter (assuming that the mean value of the jitter is zero), but a scatter about the mean is introduced by the response of the missile to the jitter signals, and an induced drag due to jitter acceleration appears.

1.2. If the system is non-linear, however, the mean miss distance is also affected in the presence of jitter, and the scatter is modified by partial saturation of the control system. The most important non-linearity (and the only one considered here) is that introduced by limiting to a safe value the lateral acceleration demanded of the missile. In the system at present envisaged, the (modified) error signal is limited rather than the control-surface deflection, in order to maintain the synthetic damping of the missile weathercock oscillation obtained by internal feedback. Near-critical damping of the weathercock mode ensures that the achieved acceleration will not exceed the demanded value.

1.3. The control surfaces are error-actuated, so that, to produce an acceleration equal to that of the beam, the missile must lag behind the beam by an amount determined by the stiffness of the missile control loop. The presence of both jitter and limits increases this lag by reducing the effective stiffness: a larger error is required to give the same mean deflection of the control surface. It is shown in this report that the non-linear system (in the sense defined above) can be analysed if certain assumptions are adopted, and if both the spectral density and the distribution of the noise are known or assumed.

1.4. The magnitude of the jitter associated with the true error signal can be controlled by the stiffness of the radar tracker. A stiff tracker implies a wide bandwidth, so that while the lag of the beam for a manoeuvring target is reduced, the mean lag of the missile behind the beam and the dispersion about this mean is adversely affected by the increased jitter. (The jitter is superposed on the true error signal, so that the total signal is clipped asymmetrically by the limits, producing a bias which opposes the true error. This effectively reduces the stiffness and therefore increases the mean lag. Thus an increased beam jitter produces not only a greater dispersion, but also an increased mean lag behind the beam). On the other hand, a narrower tracker bandwidth improves the missile response by reducing the jitter, but worsens the tracking qualities of the radar for a manoeuvring target. Similar considerations apply to the missile control-loop stiffness: increasing it reduces the mean lag but increases the dispersion and the jitter acceleration, while for a reduced stiffness the reverse is the case. On these grounds it appears that optimum values may exist for tracker and missile acceleration lags which minimise the total miss distance. If further approximations are made to simplify the equations, the optimum values and the miss distances which then obtain can be arrived at analytically.

1.5. The performance is also influenced by a number of other parameters, notably the phase-advance network constants and the damping ratios of missile and tracker; their effect is to some extent included in the analysis. The remaining parameters are determined by considerations other than that of minimising the miss distance.

2. *Analysis of the System with Jitter and Acceleration Limits.*

2.1. *The Mean and R.M.S. Control-Surface Deflections.*

The main elements of a typical beam-riding system in one plane are shown in Fig. 1. The mean positions of target, beam and missile are denoted by $\langle h_T \rangle$, $\langle h_B \rangle$ and $\langle h_M \rangle$; the G's refer to the spectral densities of stationary random processes with zero mean, and the σ's to their variances.

It is assumed that the acceleration limiting device is defined by the relations

$$V' = V, \qquad -L < V < L,$$

$$V' = L, \qquad V \geqslant L,$$

and

$$V' = -L, \qquad -L \geqslant V,$$

where V, V' are instantaneous values of input and output respectively, and L is the limiting value.

It is shown in Appendix I that, if the input of such a device consists of a steady value $\bar{x}$, together with a time function having a probability distribution $\varphi(x)$ in amplitude, the mean output $\langle y \rangle$ is given by

$$\langle y \rangle = \int_{-(L+\bar{x})}^{L-\bar{x}} (x+\bar{x})\varphi(x)dx + L \int_{L-\bar{x}}^{\infty} \varphi(x)dx - L \int_{-\infty}^{-(L+\bar{x})} \varphi(x)dx, \tag{1}$$

and the mean square output by

$$\langle y^2 \rangle = \int_{-(L+\bar{x})}^{L-\bar{x}} (x+\bar{x})^2\varphi(x)dx + L^2 \int_{L-\bar{x}}^{\infty} \varphi(x)dx + L^2 \int_{-\infty}^{-(L+\bar{x})} \varphi(x)dx. \tag{2}$$

For a normal distribution, the expressions (1) and (2) become

$$\langle y \rangle = \tfrac{1}{2}(\bar{x}+L) \operatorname{erf}\left(\frac{\bar{x}+L}{C}\right) - \tfrac{1}{2}(\bar{x}-L) \operatorname{erf}\left(\frac{\bar{x}-L}{C}\right) - \frac{C}{\sqrt{\pi}} \exp\left(-\frac{\bar{x}^2+L^2}{C^2}\right) \sinh \frac{2\bar{x}L}{C^2}, \tag{3}$$

and

$$\langle y^2 \rangle = L^2 + \tfrac{1}{2}\left(\frac{C^2}{2} + \bar{x}^2 - L^2\right)\left[\operatorname{erf}\left(\frac{\bar{x}+L}{C}\right) - \operatorname{erf}\left(\frac{\bar{x}-L}{C}\right)\right] -$$

$$- \frac{C}{\sqrt{\pi}} \exp\left(-\frac{\bar{x}^2+L^2}{C^2}\right)\left[L \cosh \frac{2\bar{x}L}{C^2} + \bar{x} \sinh \frac{2\bar{x}L}{C^2}\right], \tag{4}$$

where $1/C$ is the modulus of precision. ($C^2 = 2 \times$ variance.)

These equations can be applied to the beam rider if a steady state exists. Referring to Fig. 1, the average input to the limiter is $S\epsilon$, and the variance of the jitter is $(S\sigma)^2$. Thus the mean rudder deflection $\langle \zeta \rangle$ is given by

$$\langle \zeta \rangle = \tfrac{1}{2}(S\epsilon+g_S) \operatorname{erf}\left(\frac{S\epsilon+g_S}{S\sigma\sqrt{2}}\right) - \tfrac{1}{2}(S\epsilon-g_S) \operatorname{erf}\left(\frac{S\epsilon-g_S}{S\sigma\sqrt{2}}\right) -$$

$$- S\sigma \sqrt{\left(\frac{2}{\pi}\right)} \exp\left(-\frac{S^2\epsilon^2+g_S{}^2}{2S^2\sigma^2}\right) \sinh \frac{\epsilon g_S}{S\sigma^2}, \tag{5}$$

and the mean square rudder deflection

$$\langle \zeta^2 \rangle = g_S{}^2 + \tfrac{1}{2}(S^2\sigma^2+S^2\epsilon^2-g_S{}^2)\left[\operatorname{erf}\left(\frac{S\epsilon+g_S}{S\sigma\sqrt{2}}\right) - \operatorname{erf}\left(\frac{S\epsilon-g_S}{S\sigma\sqrt{2}}\right)\right] -$$

$$- S\sigma \sqrt{\left(\frac{2}{\pi}\right)} \exp\left(-\frac{S^2\epsilon^2+g_S{}^2}{2S^2\sigma^2}\right)\left[g_S \cosh \frac{\epsilon g_S}{S\sigma^2} + S\epsilon \sinh \frac{\epsilon g_S}{S\sigma^2}\right]. \tag{6}$$

The variance σ'^2 of the rudder deflection is by definition

$$\sigma'^2 = \langle \zeta^2 \rangle - \langle \zeta \rangle^2 \tag{7}$$

In the steady state the missile acceleration g_M is proportional to the mean rudder deflection: if $\langle\zeta\rangle$ is expressed in units of demanded acceleration, this can be written

$$g_M = R_M\ddot{\theta} + 2\dot{R}_M\dot{\theta} = \langle\zeta\rangle, \tag{8}$$

where R_M is the missile range and θ the angle of the sight line. (The rudder deflection/acceleration constant has been absorbed in the stiffness S.)

2.2. *An Approximation for the Spectral Density after the Limiter.*

Equations (5) and (8) give a relation between ϵ, the mean lag of the missile behind the beam, and σ^2, the variance of the phase-advanced jitter spectrum. The latter is a function of both the beam and missile displacement spectral densities, so that to proceed further it is necessary to find G', the spectral density after the limiter.

It is possible to obtain a formal solution for the relation between the spectral densities before and after a non-linear device, provided that the amplitude distribution is known (*see* Appendix II). For the limiter however, the solution is unamenable to further calculation in the sense required here, so that recourse has to be made to simplifying assumptions.

It will be assumed that the limiter does not affect the shape of the spectral density/frequency curve, but reduces its magnitude by the factor

$$(\sigma'/S\sigma)^2$$

this being the ratio of output to input mean square values. This gives

$$G' = S^2G\,(\sigma'/S\sigma)^2 = (\sigma'/\sigma)^2G.$$

The assumption is correct if the input spectral density is constant with frequency—the only effect of the limiter is to reduce the r.m.s. value. For other spectra the area under G'/frequency curve is correct, but the shape of the curve will be somewhat different.

Fig. 9 shows the effect of a linear rectifier when the input spectral density is constant with frequency up to ω_0, and zero thereafter. On comparing the correct output spectral density (as obtained in Appendix II) with that given by the above approximation, it will be seen that the latter is only in error in the vicinity of the cut-off frequency ω_0. Since in practice the input power spectrum will not have a sharp cut-off, the distortion is likely to be less than in the case shown.*

The amplitude distribution after the limiter is of interest in that it affects the amplitude distribution of the input *via* the main feedback loop (Fig. 1). If the distribution at the limiter input is gaussian, the output is gaussian for amplitudes less than the limits and zero outside them. The filtering action of the missile will smooth out these sharp discontinuities, so that the missile jitter will again tend towards a gaussian distribution.

---

* Since this report was written, the author's attention has been drawn to a paper by Middleton ('The Response of Biased, Saturated Linear and Quadratic Rectifiers to Random Noise.' *J. App. Physics*, Vol. 17, October, 1946), in which the effect of limiting is discussed in some detail. Middleton uses a gaussian curve for the input spectral density, as well as a gaussian amplitude distribution; with this particular input it appears that the shape of the power spectrum is not greatly affected by the limiter, even in the presence of a large d.c. term. Further, it is shown that the spread introduced by a linear rectifier is reduced if saturation occurs, as in a limiter. It appears therefore that the approximation used above is a reasonable one.

2.3. *The Missile-Beam Error, the Missile Dispersion and Jitter Acceleration.*

With the above approximation, the stiffness amplifier and acceleration limiter behave as an amplifier with a gain of σ'/σ as far as the jitter is concerned: in other words, the effective stiffness of the system is now σ'/σ instead of S.

Considering the jitter only, the forward transfer function of the missile control loop (*see* Fig. 1) can now be written as

$$\frac{\sigma'}{\sigma} X(p) Y(p),$$

where σ'/σ is the transfer function of amplifier and limiter, $X(p)$ the phase-advance network, and $Y(p)$ the missile.

The error spectral density is therefore

$$G_\epsilon = \left| \frac{1}{1 + \dfrac{\sigma'}{\sigma} X(j\omega) Y(j\omega)} \right|^2 G_B,$$

and the phase-advanced spectral density

$$G = \left| \frac{X(j\omega)}{1 + \dfrac{\sigma'}{\sigma} X(j\omega) Y(j\omega)} \right|^2 G_B$$

or

$$G = \left| \frac{X(j\omega) Z(j\omega)}{1 + \dfrac{\sigma'}{\sigma} X(j\omega) Y(j\omega)} \right|^2 G_T. \tag{9}$$

Integrating each side of equation (9) over ω, and noting that

$$\sigma^2 = \int_0^\infty G\, d\omega,$$

one obtains

$$\sigma^2 = \int_0^\infty \left| \frac{X(j\omega) Z(j\omega)}{1 + \dfrac{\sigma'}{\sigma} X(j\omega) Y(j\omega)} \right|^2 G_T\, d\omega. \tag{10}$$

From equations (5) and (8),

$$g_M = R_M \ddot{\theta} + 2\dot{R}_M \dot{\theta} = \tfrac{1}{2}(S\epsilon + g_S) \operatorname{erf}\left(\frac{S\epsilon + g_S}{S\sigma\sqrt{2}}\right) - \tfrac{1}{2}(S\epsilon - g_S) \operatorname{erf}\left(\frac{S\epsilon - g_S}{S\sigma\sqrt{2}}\right) -$$

$$- S\sigma \sqrt{\left(\frac{2}{\pi}\right)} \exp\left(-\frac{S^2\epsilon^2 + g_S^2}{2S^2\sigma^2}\right) \sinh \frac{\epsilon g_S}{S\sigma^2}. \tag{11}$$

Equations (6), (7) and (8) give

$$\sigma'^2 = g_S^2 - g_M^2 + \tfrac{1}{2}(S^2\sigma^2 + S^2\epsilon^2 - g_S^2) \left[\operatorname{erf}\left(\frac{S\epsilon + g_S}{S\sigma\sqrt{2}}\right) - \operatorname{erf}\left(\frac{S\epsilon - g_S}{S\sigma\sqrt{2}}\right)\right] -$$

$$- S\sigma \sqrt{\left(\frac{2}{\pi}\right)} \exp\left(-\frac{S^2\epsilon^2 + g_S^2}{2S^2\sigma^2}\right) \left[g_S \cosh \frac{\epsilon g_S}{S\sigma^2} + S\epsilon \sinh \frac{\epsilon g_S}{S\sigma^2}\right]. \tag{12}$$

The integration in equation (10) can be performed for known or assumed constants of the tracker, the missile and the phase-advance network, giving a relation between σ and σ'. Equations (10), (11) and (12) therefore determine σ, σ' and ϵ, the mean lag of the missile behind the beam.

The spectral density G_M of the missile displacement jitter is then given by

$$G_M = \left(\frac{\sigma'}{\sigma}\right)^2 \left| \frac{X(j\omega)\,Y(j\omega)Z(j\omega)}{1 + \frac{\sigma'}{\sigma}\, X(j\omega)\,Y(j\omega)} \right|^2 G_T,$$

from which

$$\sigma_M{}^2 = \langle h_M{}^2 \rangle - \langle h_M \rangle^2 = \left(\frac{\sigma'}{\sigma}\right)^2 \int_0^\infty \left| \frac{X(j\omega)\,Y(j\omega)Z(j\omega)}{1 + \frac{\sigma'}{\sigma}\, X(j\omega)\,Y(j\omega)} \right|^2 G_T\, d\omega\,, \tag{13}$$

where σ_M is the r.m.s. displacement of the missile about its mean position.

Finally, the missile mean square acceleration due to jitter is

$$g_J{}^2 = \left\langle \left(\frac{d^2h_M}{dt^2}\right)^2 \right\rangle - \left\langle \frac{d^2h_M}{dt^2} \right\rangle^2 = \left(\frac{\sigma'}{\sigma}\right)^2 \int_0^\infty \omega^4 \left| \frac{X(j\omega)\,Y(j\omega)Z(j\omega)}{1 + \frac{\sigma'}{\sigma}\, X(j\omega)\,Y(j\omega)} \right|^2 G_T\, d\omega\,. \tag{14}$$

Equations (10) and (14) suffice to determine ϵ, the mean lag of the missile behind the beam, and the jitter components of the missile displacement and acceleration.

2.4. *The R.M.S. Miss Distance.*

The total mean miss distance is the sum of the missile and beam lags. If θ is the sight-line angle from tracker to target, and R_T the target range, the transverse lag of the beam is $A^2 R_T \ddot{\theta}$, where A is the angular acceleration lag of the tracker:

$$\text{Beam lag} = A^2 R_T \ddot{\theta} = A^2(g_T - 2\dot{R}_T\dot{\theta}),$$

where $g_T = R_T\ddot{\theta} + 2\dot{R}_T\dot{\theta} =$ the transverse target acceleration.

The total mean miss distance D is then given by

$$\left.\begin{aligned} D &= \epsilon + A^2 R_T \ddot{\theta} \\ \text{or} \qquad D &= \epsilon + A^2(g_T - 2\dot{R}_T\dot{\theta}) \end{aligned}\right\} \tag{15}$$

where ϵ is a function of g_M: that is, of R_M, $\dot{\theta}$ and $\ddot{\theta}$.

It should be noted that, since both missile and tracker in the system considered have acceleration lags (the latter angular, the former linear), a steady state will only exist if

$$\left.\begin{aligned} \ddot{\theta} &= \text{constant} \qquad \text{(for the tracker)} \\ \text{and} \qquad R_M\ddot{\theta} + 2\dot{R}_M\dot{\theta} &= \text{constant} \qquad \text{(for the missile).} \end{aligned}\right\}$$

The dispersion about the mean is σ_M, so that the r.m.s. miss distance is

$$D_{\text{rms}} = [\sigma_M{}^2 + (\epsilon + R_T\ddot{\theta}A^2)^2]^{1/2}. \tag{16}$$

The mean and r.m.s. miss distances can therefore be calculated from equations (10) to (16) when the target manoeuvre and the system functions are defined; the required functions and parameters are:

$Z(p)$	the transfer function of the tracker, relating target angle to beam angle.
$Y(p)$	the missile transfer function relating rudder deflection and lateral acceleration.
$X(p)$	the transfer function of the phase-advance network of the missile control loop.
S	the stiffness of the missile control loop ($= 1/a^2$, where a^2 is the missile acceleration lag).
g_S	the maximum permissible lateral acceleration of the missile.
G_T	the spectral density of the primary radar jitter.
R_T	target range.
$\dot{\theta}$, $\ddot{\theta}$	the angular velocity and acceleration of the sight line induced by target manoeuvre.

The tracking servo is assumed to be sensibly linear, so that for the purpose of this analysis only the overall transfer function $Z(p)$ need be specified. The missile loop on the other hand must be specified in detail, since the position of the non-linearity within the loop is of importance.

If the missile acceleration is not limited ($g_S \to \infty$), the equations reduce to those of the linear system, giving

$$\sigma' = S\sigma$$

and

$$\text{Beam Lag} = \epsilon = \frac{g_M}{S} = a^2 g_M .$$

2.5. *The Form of the Transfer Functions.*

The form of each of the functions $X(p)$, $Y(p)$ and $Z(p)$ for the beam-riding system is well defined; the missile function is very nearly

$$Y(p) = \frac{\omega_W{}^2}{p^2(p^2 + 2u_W\omega_W p + \omega_W{}^2)} \tag{17}$$

where ω_W, u_W are the weathercock angular frquency and damping ratio respectively. This function includes the modifications to ω_W and u_W obtained by appropriate internal feedback.

The stabilising network is a phase-advance circuit of the form

$$X(p) = \frac{1 + p\tau}{1 + p\dfrac{\tau}{n}}, \tag{18}$$

where n is in the range 10 to 20. The time constant τ and the missile control-loop stiffness S govern the damping of the fully controlled motion, so that for a given degree of damping τ is determined by S.

The tracker transfer function will be taken to be of the form

$$Z(p) = \frac{1 + p\dfrac{(K+2\delta)A}{(1+2\delta K)^{1/2}}}{\left[1 + p\dfrac{KA}{(1+2\delta K)^{1/2}}\right]\left[1 + p\dfrac{2\delta A}{(1+2\delta K)^{1/2}} + p^2\dfrac{A^2}{1+2\delta K}\right]}. \tag{19}$$

The forward transfer function has a double pole at $p = 0$, so that there is no angular velocity error. A^2 is the angular acceleration lag, δ the damping ratio and K a constant of the stabilising network.

2.6. If all the parameters are known, the mean miss distance and dispersion can be found from equations (10) to (16) for a given target manoeuvre. The assumptions are:

(i) A steady state exists, i.e. the target manoeuvre is constant for a period long compared with the time lags of the system.

(ii) The noise distribution is gaussian.

(iii) The limiter reduces the magnitude of the spectral density without altering its frequency distribution.

The relations (10) to (16) form a set of simultaneous transcendental equations, so that optimum values for the parameters can only be found by numerical evaluation over a range of parameters and target manoeuvres. The remainder of this report is concerned with establishing the optimum values analytically, by using further assumptions and approximations.

3. *Choice of Parameters for the Minimum Miss Distance.*

3.1. *The Disposable Parameters.*

It is required to choose the disposable parameters so as to minimise the mean or r.m.s. miss distance.

The disposable parameters of the missile system are:

ω_W, u_W	the weathercock frequency and damping ratio—each can be adjusted by internal feedback.
ω_c, u_c	the frequency and damping of the 'control weave'.
$S(= 1/a^2)$	the loop stiffness—this largely determines ω_c.
τ, n	the time constant and attenuation constant of the phase-advance network.

Not all of these parameters are independent, and some are determined by considerations other than that of minimising the miss distance.

The tracker constants are

A^2	the angular acceleration lag
δ	the damping ratio
K	a constant of the tracker stabilising network.

3.2. *An Approximation for the Phase-Advanced Error Spectrum* {*Equation* (10)}.

If typical values are inserted in equation (10), it is found that the integral remains nearly constant when the ratio σ'/σ is varied from zero up to its expected maximum value.

Equation (10) may therefore be written

$$\sigma^2 = \int_0^\infty \left| \frac{X(j\omega)Z(j\omega)}{1 + \dfrac{\sigma'}{\sigma} X(j\omega)Y(j\omega)} \right|^2 G_T \, d\omega$$

$$\doteqdot \int_0^\infty |X(j\omega)Z(j\omega)|^2 G_T \, d\omega \,. \qquad (20)$$

The absolute maximum for σ'/σ is S—this occurs if there is no acceleration limit ($g_S \to \infty$), or no jitter ($\sigma = 0$). With practical values of jitter and missile acceleration limits the maximum value of σ'/σ will be considerably less than S—that is, the effective stiffness is considerably reduced by jitter (*see* Section 6).

The assumption is in effect that the missile jitter contributes nothing to the *phase-advanced* error jitter. This can be justified as follows: the missile will only respond to that part of the jitter spectrum within its pass-band, so that the contribution of the missile jitter to the error jitter affects only the lower part of the spectrum. On the other hand, the phase-advanced jitter consists mostly of the higher frequencies, for which the gain of the phase-advancing network is considerably greater than that for low frequencies. The missile does not respond appreciably to these higher frequencies: they are only of interest in that they saturate the control system and reduce the effective stiffness for the legitimate error signals.

The use of approximation (20) greatly simplifies the calculation, since the integral

$$\sigma^2 \doteqdot \int_0^\infty |X(j\omega)Z(j\omega)|^2 G_T \, d\omega$$

can be evaluated directly in terms of A^2, a^2, G_T, τ and n. The missile lag ϵ is then given by (11) and hence the mean miss distance D can be found from (15). The same approximation however does not hold for equation (13), so that an explicit expression for missile dispersion and r.m.s. miss distance cannot be obtained.

3.3. *An Explicit Expression for σ.*

In order to obtain an explicit expression for the miss distance D, it is necessary to evaluate the integral

$$\sigma^2 \doteqdot \int_0^\infty |X(j\omega)Z(j\omega)|^2 G_T \, d\omega \tag{20}$$

in terms of the tracker and phase-advance network parameters.

Consider first the integral

$$\Delta\omega_T = \int_0^\infty |Z(j\omega)|^2 \, d\omega ,$$

where $\Delta\omega_T$ is the noise bandwidth of the tracker. If $Z(p)$ is defined by equation (19), the integration gives

$$\Delta\omega_T = \frac{(1+2\delta K)^{1/2}}{K^4 - 2K^2(2\delta^2 - 1) + 1} \frac{\pi}{A} \left[(K+\delta)(1-2K\delta) + \frac{K^3(K+4\delta) + 2K^2 + 1}{4\delta} \right],$$

and the mean square value of the beam jitter is $\Delta\omega_T G_T$, it being assumed that G_T is constant with frequency at least over the bandwidth of the tracker. For target courses for which $\ddot{\theta}$ is constant, the mean lag of the beam behind the target is determined only by A, and is independent of δ and K. The optimum values for the latter parameters are therefore those which minimise the expression for $\Delta\omega_T$, since this condition will give the least beam jitter without affecting the beam lag.

The minimum value of $\Delta\omega_T$ occurs when $K = 0$ and $\delta = \frac{1}{2}$, in which case $\Delta\omega_T = \pi/A$. However, the parameter K is associated with a time lag in the tracker, and cannot therefore be made zero. For a given K, the optimum value of δ (i.e. that for which $\Delta\omega_T$ is a minimum) is given by

$$\delta_{\text{opt}} = \frac{1}{2} + \frac{1}{4}K + \frac{9}{16}K^2 - \frac{1}{8}K^3 - \frac{81}{2J6}K^4 + \ldots$$

Taking $K = 0 \cdot 2$ as a reasonable value, this gives $\delta_{\text{opt}} = 0 \cdot 57$, and $\Delta\omega_T = 1 \cdot 16\, \pi/A$.

Thus $\delta = 0{\cdot}57$ is the optimum damping ratio of the tracker (with $K = 0{\cdot}2$) for constant $\ddot{\theta}$ targets. In order however to compare the numerical results of the theory developed here with the simulator results discussed in Section 4, the values $K = 0{\cdot}2$, $\delta = 1$, will be taken, since these are the values used in the simulator.

With these values, $\Delta\omega_T = 1{\cdot}28\ \pi/A$, so that the noise bandwidth of the tracker is 10% greater than the minimum bandwidth ($\delta = 0{\cdot}57$). However, it is shown later (Section 3.4) that the minimum mean miss distance varies as the two-sevenths power of the jitter spectral density; the miss distance is therefore hardly affected by changing δ from $0{\cdot}57$ to 1.

It should be emphasised that this applies only to constant $\ddot{\theta}$ targets: the miss distance against target courses which generate higher derivatives of θ may be more critically dependent on the value of δ.

The noise bandwidth of the combination of tracker and phase-advance network is

$$\Delta\omega = \int_0^\infty |X(j\omega)Z(j\omega)|^2 \, d\omega \, .$$

Taking equations (18) and (19) as representing $X(p)$ and $Z(p)$ respectively and putting $K = 0{\cdot}2$, $\delta = 1$, this gives on integration:

$$\Delta\omega = \frac{\pi n^2}{A}\left[\frac{0{\cdot}617(35\tau^2 - A^2)}{(n^2A^2 - 35\tau^2)} - \frac{118nA\tau^3(0{\cdot}29\tau^2 - n^2A^2)}{(35\tau^2 - n^2A^2)\,(1{\cdot}4\tau^2 - n^2A^2)^2} + \right.$$
$$\left. + \frac{3{\cdot}08(A^2 - 2{\cdot}52\tau^2)}{(n^2A^2 - 1{\cdot}4\tau^2)} - \frac{1{\cdot}19(A^2 - 1{\cdot}4\tau^2)\,(n^2A^2 - 4{\cdot}45\tau^2)}{(n^2A^2 - 1{\cdot}4\tau^2)^2}\right] . \qquad (21)$$

If the primary jitter spectrum G_T can be considered flat, then

$$\sigma^2 = G_T \Delta\omega \, , \qquad (22)$$

where the approximation of equation (20) has been used.

The expression

$$\Delta\omega = 30\,\frac{\tau^2}{A^3} \qquad (23)$$

is a rough approximation (10 to 15%) to equation (21) over the normal range of A and τ, taking $n = 20$. Using this value in equation (22) gives

$$\sigma = \sqrt{(30G_T)}\,\frac{\tau}{A^{3/2}} \, . \qquad (24)$$

As was indicated in Section 3.1, the phase-advance time constant τ is intimately related to S, the missile control-loop stiffness, in order to maintain adequate damping. The relationship can be derived as follows:

For the linear system,

$$h_M = SX(p)\,Y(p)\,(h_B - h_n)$$

or

$$h_M = \frac{SX(p)\,Y(p)}{1 + SX(p)\,Y(p)}\,h_B \, ,$$

where h_M, h_B are missile and beam displacements (*see* Fig. 1).

Substituting for $Y(p)$ and $X(p)$ from equations (17) and (18), and neglecting the impurity term in the latter ($n \to \infty$),

$$h_M = \frac{S\omega_W{}^2(1+p\tau)}{p^2(p^2+2u_W\omega_W p+\omega_W{}^2) + S\omega_W{}^2(1+p\tau)}\, h_B$$

$$= \frac{S\omega_W{}^2(1+p\tau)}{(p^2+2u_W{}'\omega_W{}'p+\omega_W{}'^2)\,(p^2+2u_C\omega_C p+\omega_C{}^2)}\, h_B\,.$$

Equating coefficients in the denominator of the last two expressions,

$$\left.\begin{aligned} S\omega_W{}^2 &= \omega_W{}'^2\omega_C{}^2 \\ \text{and} \qquad S\omega_W{}^2\tau &= 2u_W{}'\omega_W{}'\omega_C{}^2 + 2u_C\omega_C\omega_W{}'^2\,. \end{aligned}\right\} \tag{25}$$

The frequency and damping of the $\omega_W{}'$ mode is very similar to the weathercock mode, this being hardly affected by closing the control loop. Approximately therefore $u_W{}' = u_W$ and $\omega_W{}' = \omega_W$. Substituting in equation (25),

$$\omega_C{}^2 = S \text{ or } \omega_C = \frac{1}{a},$$

and

$$\tau = \frac{2u_W}{\omega_W} + 2u_C a\,. \tag{26}$$

Inserting this value in equation (24) gives

$$\sigma = \sqrt{(30G_T)}\left(\frac{2u_W}{\omega_W} + 2u_C a\right) A^{3/2}\,. \tag{27}$$

3.4. *The Minimum Mean Miss Distance.*

Equations (11), (27) and (15) enable the mean miss distance D to be found, subject to the approximations already noted. With one further approximation it is possible to deduce analytically the values of the parameters which give the minimum mean miss distance, without regard to the dispersion about this mean.

The relation expressed by equation (11) is shown graphically in Fig. 3, where g_M/g_S is plotted against $S\epsilon/g_S$ with $\epsilon/\sigma\sqrt{2}$ as a parameter; and also in Fig. 4, which shows $\epsilon/\sigma\sqrt{2}$ as a function of $S\sigma\sqrt{2}/g_S$ with g_M/g_S as the parameter. Each curve of Fig. 3 is asymtotic to erf $(\epsilon/\sigma\sqrt{2})$, so that, for infinite stiffness,

$$\operatorname{erf}\frac{\epsilon}{\sigma\sqrt{2}} = \frac{g_M}{g_S}\,. \tag{28}$$

The curves show that, for constant σ, the missile lag ϵ decreases monotonically with increasing stiffness, and that the minimum value is approached very rapidly. This is still true when σ is given by equation (27), since σ decreases with increasing stiffness for all values of A.

Equation (28) is therefore a good approximation to equation (11) over the range of stiffness which gives the minimum ϵ; if the working point lies in the curved region, ϵ can be decreased appreciably by increasing the stiffness, i.e. by moving into the flat region where the approximation holds.

From equations (15) and (28)

$$\operatorname{erf}\left[\frac{D - A^2R_T\ddot{\theta}}{\sigma\sqrt{2}}\right] = \frac{g_M}{g_S}\,.$$

On substituting for σ from equation (27),

$$\operatorname{erf}\left[\frac{(D - A^2 R_T \ddot{\theta}) A^{3/2}}{\sqrt{(60 G_T)} \left(\dfrac{2u_W}{\omega_W} + 2u_C a\right)}\right] = \frac{g_M}{g_S},$$

or

$$D = \left[\sqrt{(60 G_T)} \left(\frac{2u_W}{\omega_W} + 2u_C a\right) \operatorname{erf}^{-1} \frac{g_M}{g_S}\right] A^{-3/2} + A^2 R_T \ddot{\theta}. \tag{29}$$

In this expression, the mean miss distance D is obviously a minimum when u_W, u_C and a are as small as possible, and ω_W large, i.e. the miss distance is least for high weathercock and weave frequencies and light damping of both modes. The latter result is consistent with the steady-state assumption implied in the analysis, but, as was the case with the tracker damping discussed earlier (Section 3.3), light damping ratios are unacceptable for other reasons—e.g. the weathercock damping must be near critical for the limiting system to be effective.

The optimum value for A is found from $\partial D/\partial A = 0$, which gives

$$A^2 = \frac{3}{7} \frac{D}{R_T \ddot{\theta}}.$$

Inserting this value in (29)

$$\left.\begin{aligned} D_{\min} &= 6 \cdot 4 \left[\left(\frac{2u_W}{\omega_W} + 2u_C a\right) \sqrt{(G_T)}\, (R_T \ddot{\theta})^{3/4} \operatorname{erf}^{-1} \frac{g_M}{g_S}\right]^{4/7} \\ A_0^2 &= \frac{3}{7} \frac{D_{\min}}{R_T \ddot{\theta}} \end{aligned}\right\} \tag{30}$$

where $D_{\min}$ and A_0 denote the values of D and A which satisfy (29) and $\partial D/\partial A = 0$.

The displacement jitter spectral density G_T can be written in terms of the angular spectral density J_T:

$$G_T = R_M^2 J_T = R_T^2 J_T,$$

since $R_M = R_T$ at strike. Also

$$g_M = R_M \ddot{\theta} + 2\dot{R}_M \dot{\theta}.$$

Equation (30) then becomes

$$\left.\begin{aligned} D_{\min} &= 6 \cdot 4\, R_T \ddot{\theta}^{3/7} J_T^{2/7} \left[\left(\frac{2u_W}{\omega_W} + 2u_C a\right) \operatorname{erf}^{-1} \left(\frac{R_M \ddot{\theta} + 2\dot{R}_M \dot{\theta}}{g_S}\right)\right]^{4/7} \\ A_0^2 &= \frac{3}{7} \frac{D_{\min}}{R_T \ddot{\theta}}. \end{aligned}\right\} \tag{31}$$

3.5. *Optimum Values of a^2 and A^2.*

For each value of a^2, therefore, there is an optimum value of the tracker lag (A^2) which minimises the mean miss distance: the minimum decreases with decreasing a^2, reaching the absolute minimum for infinite missile loop stiffness ($a^2 = 0$).

The above analysis breaks down for very stiff systems, since the approximation (20) is no longer valid; also, the system could not be made stable for very high loop gains.

It would appear therefore that, from a consideration of mean miss distance only, the missile stiffness should be as great as is consistent with stability; there is then a corresponding value for A^2 which gives the minimum mean miss distance, and this value is a function of target manoeuvre.

4. *Three Examples: Comparison with Simulator Results.*

4.1. Three numerical examples are given in Table 2. The constants have been chosen to agree with those for which simulator results have been obtained. The aerodynamic constants are shown in Table 1, but for this analysis the missile is completely specified by its (modified) weathercock frequency and damping.

With $\kappa_W = 1$, $\omega_W = 16$, and $\kappa_C = 0 \cdot 5$, equation (26) gives

$$\tau = 0 \cdot 125 + a. \tag{32}$$

This is plotted in Fig. 2, together with the simulator values of τ: equation (32) expresses the observed relation between τ and a fairly accurately.

The target manoeuvre has been taken to be such that

$$R_T = 100\,000 \text{ ft}, \qquad R_T\ddot{\theta} = 2g,$$

and

$$R_T\ddot{\theta} \gg 2\dot{R}_M\dot{\theta},$$

i.e. the target has a constant acceleration of $2g$ perpendicular to the beam.

TABLE 1

Aerodynamic Constants

$\dfrac{Y_v}{M}$	$\dfrac{Y_r}{M}$	$\dfrac{Y_\zeta}{M}$	$\dfrac{N_v}{C}$	$\dfrac{N_r}{C}$	$\dfrac{N_\zeta}{C}$
$\dfrac{1}{\text{sec}}$	$\dfrac{\text{ft}}{\text{rad. sec}}$	$\dfrac{\text{ft}}{\text{rad. sec}^2}$	$\dfrac{\text{rad}}{\text{ft. sec}}$	$\dfrac{1}{\text{sec}}$	$\dfrac{1}{\text{sec}^2}$
-1	$2 \cdot 4$	800	1/15	-1	-200

4.2. In the first example the missile acceleration is limited to $10g$, and the angular spectral density of the jitter is $0 \cdot 04$ mil^{2}sec. The minimum mean miss distance and the optimum value of A^2, obtained from equations (31), are shown in rows (c) and (d) of Table 2 for various values of a^2; rows (e) and (f) show how the miss distance is distributed between missile lag and beam lag.

The variation of $D_{\min}$ with a^2 is shown graphically in Fig. 5. Doubling the spectral density (Example III) only increases the minimum miss distance by about 20%, while a decrease of about 40% is obtained by doubling the missile acceleration limits (Example II).

The parameter $S\epsilon/g_S$ is given in row (h), Table 2; comparison with Fig. 3 shows that the approximation

$$\operatorname{erf} \frac{\epsilon}{\sigma\sqrt{2}} = \frac{g_M}{g_S} \tag{28}$$

is justified, except in the case of the last three columns for Example II: these points lie in the curved region, so that the approximation gives optimistic results. In this relatively linear system ($20g$ limits), both the tracker and the missile can be appreciably stiffened to reduce the minimum *mean* miss distance.

TABLE 2

Miss Distances against a Manoeuvring Target

Target Manoeuvre: $R_T\ddot{\theta} = 2g$. Target Range: 100 000 ft

		EXAMPLE I				
		Jitter Spectral Density $0 \cdot 04$ mil²sec Missile Acceleration Limit $10g$				
(a) Missile acceleration lag [sec²]	a^2	0·1	0·2	0·3	0·4	0·5
(b) Phase-advance time constant (= $0 \cdot 125 + a$) [sec]	τ	0·44	0·57	0·67	0·76	0·83
(c) Optimum tracker acceleration lag [sec²]	A_0^2	0·332	0·385	0·421	0·450	0·476
(d) Minimum mean miss distance [ft]	$D_{\min}$	49	57	62	67	71
(e) Mean lag of missile behind beam [ft]	ϵ	28	33	35	38	41
(f) Mean lag of beam behind target [ft]	$A_0^2 R_T \ddot{\theta}$	21	24	27	29	30
(g) R.M.S. phase-advanced jitter [ft]	σ	111	128	140	150	159
(h) Ratio of mean limiter input to limiting acceleration	$\frac{S\epsilon}{g_S}$	0·885	0·514	0·374	0·298	0·254
(i) Ratio of r.m.s. limited jitter to limiting acceleration	$\frac{\sigma'}{g_S}$	0·90	0·84	0·78	0·74	0·70
(j) Effective stiffness for jitter [ft/sec²/ft]	$\frac{\sigma'}{\sigma}$	2·7	2·1	1·78	1·57	1·41
(k) Nominal stiffness [ft/sec²/ft]	S (= $1/a^2$)	10	5	3·3	2·5	2
(l) Missile dispersion [ft]	σ_M	78	66	60	57	54
(m) Total r.m.s. miss distance $(D^2_{\min} + \sigma_M^2)^{1/2}$ [ft]	$D_{\text{r.m.s.}}$	92	87	86	87	88

TABLE 2—*continued*

		EXAMPLE II Jitter Spectral Density 0·04 mil²sec Missile Acceleration Limit 20*g*				
(a) Missile acceleration lag [sec²]	a^2	0·1	0·2	0·3	0·4	0·5
(b) Phase-advance time constant (= 0·125 + *a*) [sec]	τ	0·44	0·57	0·67	0·76	0·83
(c) Optimum tracker acceleration lag [sec²]	A_0^2	0·223	0·258	0·283	0·303	0·320
(d) Minimum mean miss distance [ft]	$D_{\min}$	33	38	42	45	48
(e) Mean lag of missile behind beam [ft]	ϵ	19	22	24	26	27
(f) Mean lag of beam behind target [ft]	$A_0^2 R_T \ddot{\theta}$	14	16	18	19	21
(g) R.M.S. phase-advanced jitter [ft]	σ	148	173	190	202	214
(h) Ratio of mean limiter input to limiting acceleration	$\frac{S\epsilon}{g_S}$	0·293	0·172	0·125	0·100	0·085
(i) Ratio of r.m.s. limited jitter to limiting acceleration	$\frac{\sigma'}{g_S}$	0·88	0·78	0·70	0·62	0·57
(j) Effective stiffness for jitter [ft/sec²/ft]	$\frac{\sigma'}{\sigma}$	3·8	2·88	2·35	1·96	1·70
(k) Nominal stiffness [ft/sec²/ft]	S $(= {}^1/a^2)$	10	5	3·3	2·5	2
(l) Missile dispersion [ft]	σ_M	88	71	64	60	57
(m) Total r.m.s. miss distance $(D^2_{\min} + \sigma_M{}^2)^{1/2}$ [ft]	$D_{\mathrm{r.m.s.}}$	94	81	76	75	74

TABLE 2—*continued*

		EXAMPLE III Jitter Spectral Density 0·08 mil²sec Missile Acceleration Limit 10*g*				
(a) Missile acceleration lag [sec²]	a^2	0·1	0·2	0·3	0·4	0·5
(b) Phase-advance time constant (= 0·125 + *a*) [sec]	τ	0·44	0·57	0·67	0·76	0·83
(c) Optimum tracker acceleration lag [sec²]	A_0^2	0·404	0·470	0·514	0·548	0·580
(d) Minimum mean miss distance [ft]	$D_{\min}$	60	70	76	82	87
(e) Mean lag of missile behind beam [ft]	ϵ	34	40	43	47	50
(f) Mean lag of beam behind target [ft]	$A_0^2 R_T \ddot{\theta}$	26	30	33	35	37
(g) R.M.S. phase-advanced jitter [ft]	σ	135	157	171	184	194
(h) Ratio of mean limiter input to limiting acceleration	$\frac{S\epsilon}{g_S}$	1·07	0·625	0·454	0·366	0·309
(i) Ratio of r.m.s. limited jitter to limiting acceleration	$\frac{\sigma'}{g_S}$	0·91	0·86	0·81	0·78	0·75
(j) Effective stiffness for jitter [ft/sec²/ft]	$\frac{\sigma'}{\sigma}$	2·15	1·75	1·52	1·35	1·24
(k) Nominal stiffness [ft/sec²/ft]	S $(= 1/a^2)$	10	5	3·3	2·5	2
(l) Missile dispersion [ft]	σ_M	110	90	83	81	78
(m) Total r.m.s. miss distance $(D^2_{\min} + \sigma_M{}^2)^{1/2}$ [ft]	$D_{\text{r.m.s.}}$	125	113	112	114	115

The optimum value of A^2 is not very critical; the variation of D with A^2 is illustrated in Fig. 6 for $a^2 = 0 \cdot 3$, Example I. For large values of A^2 the approximation (28) breaks down, and the miss distance increases rather more rapidly in this region than is indicated on the diagram.

4.3. Simulator results for the above three examples are compared in Table 3 with those obtained from the present theory. In the simulator results an optimum value is given for both a^2 and A^2, and these are shown in the simulator columns for each example. The theory does not indicate an optimum value for a^2 other than zero (i.e. the missile control-loop stiffness should be as high as stability considerations allow), but for comparison the simulator values of this parameter have been taken. The second column shows the mean miss distance as given by equation (29) for the simulator values of a^2 and A^2, while the third column gives the minimum mean miss distance and the optimum A^2 for the given a^2, from equations (30).

TABLE 3

Comparison of Simulator and Theoretical Results

	Example I			Example II			Example III		
		Theory			Theory			Theory	
	Simulator (optimum)	{Equation (29)}	Optimum {equations (30)}	Simulator (optimum)	{Equation (29)}	Optimum {equations (30)}	Simulator (optimum)	{Equation (29)}	Optimum {equations (30)}
a^2 sec^2	0·448	0·448	0·448	0·257	0·257	0·257	0·591	0·591	0·591
A^2 sec^2	0·269	0·269	0·462	0·154	0·154	0·268	0·355	0·355	0·596
Miss dist. D ft	66	76	69	40	45	40	87	100	89

In all three cases there is close agreement for the minimum miss distances; the theoretical values of A^2 for which they occur are all somewhat higher than the corresponding simulator values. Also the theory indicates that the mean miss distance can be reduced by increasing the missile control-loop stiffness, subject to the conditions noted in Section 3.5.

The simulator results are for a fixed ratio of weathercock-like to weave frequencies. Since the weave frequency is very nearly $1/a$, a change of stiffness implies a change of weathercock frequency to maintain the constant ratio. In the theory the weathercock frequency is fixed, so that the ratio alters when the stiffness is varied, and the two sets of results—simulator and theoretical—are therefore not strictly comparable.

The effect of this variation should however be small, since the weathercock frequency ω_W can vary appreciably without greatly altering either τ or the mean miss distance {cf. equations (26) and (31)}.

5. *Miss Distance for a Distribution of Accelerating Targets.*

5.1. Equations (31) can be further simplified by making use of the approximation

$$\operatorname{erf}^{-1}\frac{g_M}{g_S} = 0\cdot 9\,\frac{g_M}{g_S},$$

which holds over the range $0 \leqslant g_M/g_S < 0\cdot 4$. Higher values of g_M/g_S are of no interest, since in the presence of the degree of jitter envisaged the miss distances are excessive: that is, the missile must be able to withstand much more than the expected legitimate accelerations demanded of it.

With this approximation, equations (31) reduce to

$$\left.\begin{aligned} D_{\min} &= 6R_T\ddot{\theta}^{3/7}J_T^{2/7}\left[\left(\frac{2u_W}{\omega_W}+2u_Ca\right)\left(\frac{R_M\ddot{\theta}+2\dot{R}_M\dot{\theta}}{g_S}\right)\right]^{4/7} \\ A_0^2 &= 2\cdot 56\,J_T^{2/7}\left[\left(\frac{2u_W}{\omega_W}+2u_Ca\right)\left(R_M+2\dot{R}_M\frac{\dot{\theta}}{\ddot{\theta}}\right)\Big/g_S\right]^{4/7}. \end{aligned}\right\} \tag{33}$$

5.2. The above equations (33) show that the optimum value for the tracker acceleration lag depends on the ratio $\dot{\theta}/\ddot{\theta}$ and on the range of engagement R_T ($= R_M$ at strike), so that in order to select an overall optimum it is necessary to assess the distributions of $\dot{\theta}$ and $\ddot{\theta}$ for likely target courses.

For the particular class of targets for which

$$R_T\ddot{\theta} \gg 2\dot{R}_M\dot{\theta},$$

equations (33) give

$$\left.\begin{aligned} D_{\min} &= 6R_T\ddot{\theta}J_T^{2/7}\left[\left(\frac{2u_W}{\omega_W}+2u_Ca\right)\frac{R_T}{g_S}\right]^{4/7}, \\ A_0^2 &= 2\cdot 56\,J_T^{2/7}\left[\left(\frac{2u_W}{\omega_W}+2u_Ca\right)\frac{R_T}{g_S}\right]^{4/7}, \end{aligned}\right\} \tag{34}$$

which show that for a fixed engagement range the optimum tracker acceleration lag is independent of the target acceleration perpendicular to the beam.

The minimum mean miss distance is now directly proportional to target acceleration $R_T\ddot{\theta}$, so that if a distribution of targets is considered for which $R_T\ddot{\theta} \gg 2\dot{R}_M\dot{\theta}$, the miss distances will have the same distribution. If, for example, the target acceleration distribution is gaussian with variance σ_T^2,

$$\text{Mean (Mean Miss Dist.)} = \sqrt{\left(\frac{2}{\pi}\right)}\,6J_T^{2/7}\left[\left(\frac{2u_W}{\omega_W}+2u_Ca\right)R_T\right]^{4/7}\sigma_T$$

and

$$\text{R.M.S. (Mean Miss Dist.)} = 6J_T^{2/7}\left[\left(\frac{2u_W}{\omega_W}+2u_Ca\right)R_T\right]^{4/7}\sigma_T.$$

Thus the values quoted for $D_{\min}$ in Table 2 may be regarded as r.m.s. mean miss distances against a distribution of target accelerations with a variance of $2g$, where each member of the target population is assumed to be such that $R_T\ddot{\theta} \gg 2\dot{R}_M\dot{\theta}$, and to have a steady acceleration which persists for a sufficient duration before impact to allow the tracker and missile control systems to have reached the steady state for which the analysis holds. In addition, there exists at the input to the system a random signal with spectral density J_T, which may be attributed either to target motion or to radar jitter, or a combination of both.

The r.m.s. mean miss distance in this context is not the same as the r.m.s. miss distance when attacking a single manoeuvring target in the presence of jitter: this is discussed in the next paragraph.

6. *The Jitter Components of Missile Motion.*

6.1. Equations (32) give the minimum mean miss distance in the presence of jitter and of acceleration limits, and the value of A^2 for which this minimum occurs. There will also be a dispersion σ_M about the mean given by

$$\sigma_M{}^2 = \left(\frac{\sigma'}{\sigma}\right)^2 \int_0^\infty \left| \frac{X(j\omega)\,Y(j\omega)Z(j\omega)}{1 + \dfrac{\sigma'}{\sigma}\,X(j\omega)\,Y(j\omega)} \right|^2 G_T\,d\omega\,, \tag{13}$$

and an acceleration dispersion g_J, where

$$g_J{}^2 = \left(\frac{\sigma'}{\sigma}\right)^2 \int_0^\infty \omega^4 \left| \frac{X(j\omega)\,Y(j\omega)Z(j\omega)}{1 + \dfrac{\sigma'}{\sigma}\,X(j\omega)\,Y(j\omega)} \right|^2 G_T\,d\omega\,. \tag{14}$$

Equations (13) and (14) are of the same form as for the linear system, with σ'/σ replacing the missile stiffness S. The quantity σ'/σ is therefore the effective stiffness: that is, the missile jitter in the presence of limits and stiffness S is the same as would be obtained without limits but with the reduced stiffness σ'/σ.

The ratio σ'/σ can be evaluated by using equations (11) and (12). The curves of Fig. 7 are derived from these equations; σ'/g_S is plotted as a function of $S\epsilon/g_S$ with $\epsilon/\sigma\sqrt{2}$ as a parameter.

The evaluation of σ'/σ is illustrated in Table 2 for each of the three examples. The missile lag ϵ is obtained from

$$\epsilon = D_{\min} - A_0{}^2 R_T \ddot{\theta}\,, \tag{15}$$

so that $S\epsilon/g_S$ is known. ($S = 1/a^2$).
Also

$$\frac{\epsilon}{\sigma\sqrt{2}} = \mathrm{erf}^{-1}\frac{g_M}{g_S} \doteqdot 0{\cdot}9\,\frac{g_M}{g_S}\,. \tag{28}$$

From (15) and (28),

$$\sigma = \frac{1}{0{\cdot}9\,\sqrt{2}}\,\frac{g_S}{g_M}\,(D_{\min} - A_0{}^2 R_T \ddot{\theta})\,. \tag{35}$$

The parameters $S\epsilon/g_S$ and $\epsilon/\sigma\sqrt{2}$ suffice to determine σ'/g_S from Fig. 7: and this value together with equation (35) gives the effective stiffness σ'/σ.

Table 2, row (j), shows the effective stiffness for each value of a^2, when the mean miss distance has been minimised according to equations (31). For comparison, the nominal stiffness ($1/a^2$) is given in row (k). The reduction in stiffness is greatest in Example III (large jitter and $10g$ limits), and least in II (half the jitter and $20g$ limits), while I is the intermediate case.

6.2. The missile dispersion σ_M and jitter acceleration g_J can now be obtained from equations (13) and (14), which can be evaluated either with a simulator (without limits) or graphically. The results of graphical integration for σ_M are tabulated in row (l) of Table 2. The dispersion decreases and $D_{\min}$ increases with increasing a^2, and there is an optimum value of a^2 which minimises the r.m.s. miss distance:

$$D_{\mathrm{rms}} = [D_{\min}{}^2 + \sigma_M{}^2]^{1/2}. \tag{36}$$

This gives optimum values for both the tracker and the missile acceleration lags. The minimum r.m.s. miss distance {row (m)} occurs when a^2 is in the region $0{\cdot}2$ to $0{\cdot}4$, in all three cases: but the miss distance is not very sensitive to variations of A^2 and a^2 about their optimum values.

The above procedure minimises the r.m.s. miss distance when the mean miss distance has itself been minimised with respect to A^2.

A study of Fig. 7 shows that over the normal range of values σ'/g_S depends only on the ratio $(S\epsilon/g_S)/(\epsilon/\sigma\sqrt{2})$, that is on $S\sigma\sqrt{2}/g_S$. The relation is shown in Fig. 8, where σ'/g_S is plotted against $S\sigma\sqrt{2}/g_S$.

From equation (27),

$$\frac{S\sigma\sqrt{2}}{g_S} = \sqrt{(60G_T)}\left(\frac{2u_W}{\omega_W} + 2u_C a\right)\Big/ a^2 g_S A_0{}^{3/2}. \tag{37}$$

It was shown in Section 5.2 that the optimum tracker acceleration lag is independent of the target acceleration if $R_T\ddot{\theta} \gg 2\dot{R}_M\dot{\theta}$. It follows from equation (37) and Fig. 8 that σ'/σ, and hence the missile dispersion and jitter acceleration, are also independent of the mean target acceleration.

The values of σ'/σ and σ_M given in Table 2 are therefore applicable to any target manoeuvre for which $R_T\ddot{\theta} \gg 2\dot{R}_M\dot{\theta}$, provided that g_M/g_S is not greater than about $0{\cdot}4$.

7. *The Miss Distance in Three Dimensions.*

7.1 The discussion so far has been restricted to two dimensions, but the results obtained can readily be extended to cover the three-dimensional case.

Let the beam angle θ be measured in the plane in which the beam is accelerating; this involves no loss of generality if $R_T\ddot{\theta}$ is taken to be the resultant lag due to azimuth and elevation tracking lags. The plane thus defined is parallel to the missile fly-plane. (Without acceleration limits the planes are coincident.)

Suppose that the pitch plane of the (cruciform) missile makes an angle φ with the fly-plane. Then the accelerations demanded in pitch and yaw are

$$g_{Mz} = g_M \cos\varphi,$$

$$g_{My} = g_M \sin\varphi.$$

It will be assumed that g_S refers to the safe acceleration limit in each plane, i.e. a maximum of $\sqrt{2}g_S$ is allowed in a bisecting plane. Equation (28) then gives

$$\operatorname{erf}\frac{\epsilon_z}{\sqrt{2}\sigma_z} = \frac{g_M\cos\varphi}{g_S},$$

and

$$\operatorname{erf}\frac{\epsilon_y}{\sqrt{2}\sigma_y} = \frac{g_M\sin\varphi}{g_S}.$$

Making use of approximation (20), $\sigma_z \doteqdot \sigma_y = \sigma$. Then the total missile lag is

$$(\epsilon_z^2 + \epsilon_y^2)^{1/2} = \sqrt{2}\,\sigma \left[\left(\mathrm{erf}^{-1}\frac{g_M \cos\varphi}{g_S}\right)^2 + \left(\mathrm{erf}^{-1}\frac{g_M \sin\varphi}{g_S}\right)^2\right]^{1/2}. \tag{38}$$

This expression averaged over φ gives the average missile lag.

If as in Section 5 the approximation $\mathrm{erf}^{-1}x = 0{\cdot}9x\,(x < 0{\cdot}4)$ is used equation (38) reduces to

$$\begin{aligned}(\epsilon_z^2 + \epsilon_y^2)^{1/2} &= 0{\cdot}9\,\sqrt{2}\,\sigma g_M/g_S \\ &= \epsilon\text{, from (28)},\end{aligned}$$

and therefore the mean miss distance D' is given by

$$D' = \epsilon + A^2 R_T \ddot{\theta},$$

so that the mean miss distance is identical with that for two-dimensional case.

7.2. The dispersions σ_{Mz} and σ_{My} in the two planes will not in general be the same, since they depend on ϵ_z and ϵ_y. The equation for the pitch plane corresponding to (12) is

$$\sigma_z' = g_S^2 - g_M^2\cos^2\varphi + \tfrac{1}{2}(S^2\sigma_z^2 + S^2\epsilon_z^2 - g_S^2)\left[\mathrm{erf}\left(\frac{S\epsilon_z + g_S}{S\sigma_z\sqrt{2}}\right) - \mathrm{erf}\left(\frac{S\epsilon_z - g_S}{S\sigma_z\sqrt{2}}\right)\right] -$$

$$- S\sigma_z\sqrt{\left(\frac{2}{\pi}\right)}\exp\left(-\frac{S^2\epsilon_z^2 + g_S^2}{2S^2\sigma_z^2}\right)\left[g_S\cosh\frac{\epsilon_z g_S}{S\sigma_z^2} + S\epsilon_z\sinh\frac{\epsilon_z g_S}{S\sigma_z^2}\right],$$

with a similar equation for σ_y'. The ratios σ_z'/σ_z and σ_y'/σ_y thus obtained enable the dispersions σ_{Mz} and σ_{My} to be found from equation (13).

If the stiffness, phase advance, etc. are identical in each channel any difference between σ_{Mz} and σ_{My} will be due only to the inequality of ϵ_z and ϵ_y. However, it was shown in Section 6.2 that the missile dispersion is rather independent of the mean acceleration, and therefore of ϵ_z and ϵ_y. Hence

$$\sigma_{Mz} \doteqdot \sigma_{My} \doteqdot \sigma_M,$$

so that the total scatter is

$$(\sigma_{Mz}^2 + \sigma_{My}^2)^{1/2} = \sqrt{2}\,\sigma_M,$$

where σ_M is the two-dimensional dispersion.

7.3. The above results give for the total r.m.s. miss distance

$$D_{\mathrm{rms}}' = [D^2 + 2\sigma_M^2]^{1/2}$$

$$D_{\mathrm{rms}}' = [D^2_{\mathrm{rms}} + \sigma_M]^{1/2}$$

where D, D_{rms} and σ_M are the values defined above (Section 2.4) for the two-dimensional case.

8. *Summary of Assumptions and Approximations.*

8.1. The approximations made in the foregoing paragraphs are reviewed below. Three assumptions have been adopted to arrive at a set of equations which describe the non-linear system; they are as follows:

(i) A steady state exists. This is satisfied if the mean target acceleration persists for, say, three or four periods of the control weave frequency.

(ii) The noise distribution at the input to the limits is gaussian. The distribution must be specified if account is to be taken of the limits, and this seems a reasonable choice.

(iii) The limiter reduces the magnitude of the Spectral Density without altering its frequency distribution. The output variance σ', given by equation (12), defines $\int_0^\infty G' \, d\omega$, so that the assumption serves to define G', the spectral density after limiting. The error incurred can be found by the method of Appendix II: its effect on results deduced from an analysis based on the assumption can only be gauged by experiment.

These three assumptions lead to equations (10) to (16), from which the mean and r.m.s. miss distances, the missile jitter displacement and jitter acceleration can be determined. The equations are given in terms of R_T, $\dot{\theta}$ and $\ddot{\theta}$, which are determined by the target motion.

8.2. In order to find analytically the best values for the main parameters, it is necessary to introduce further approximations which simplify the equations. These are given below.

(iv) The spectrum of the phase-advanced error is unaffected by the jitter of the missile. This is discussed in Section 3.2, and leads to equation (20).

(v) The spectral density of the primary jitter G_T is constant over the frequency range of interest. This is the assumption currently adopted in the absence of more precise information. If G_T has some other distribution, the appropriate function must be included in the integrals of equations (13), (14) and (20).

These two approximations allow the calculation of the phase-advanced error spectrum from the noise bandwidth of tracker plus phase-advanced network. The resulting expression (21) leads to high-order algebraic equations for the optimum values, so that the approximation

(vi) $\sigma \doteqdot \sqrt{(30G_T)}\tau/A^{3/2}$ is used. The additional approximation

(vii) erf $\epsilon/\sigma\sqrt{2} \doteqdot g_M/g_S$ for equation (11) leads to a solution for the optimum value of A^2 for the minimum mean miss distance. These in turn enable the effective stiffness to be obtained, from which the dispersion and acceleration due to jitter can be found for each value of a^2. The latter can then be chosen to minimise the r.m.s. miss-distance.

9. *Conclusions.*

9.1. The methods adopted for dealing with the non-linear system appear to give reasonable results—the specific examples evaluated agree quite well with simulator estimates. The agreement is sufficiently close to allow the extension of the method to similar problems—e.g. the effect of further non-linearities in the system—with the expectation of fairly accurate results, using the same basic assumptions.

9.2. The results obtained show that, while optimum values exist for most of the parameters considered, they can be varied considerably without appreciably affecting the r.m.s. miss distance at least against targets for which $\ddot{\theta}$ is constant. This indicates that the system constants can be chosen from considerations other than that of minimising the miss distance.

9.3. If the values assumed for the jitter spectral density and for the target manoeuvre are representative, the theory indicates that the ratio of the missile acceleration limit to the maximum legitimate acceleration demand (g_S/g_M) should not be less than about 5, in order to maintain a reasonable performance against targets whose courses demand this maximum acceleration from the missile. A smaller ratio leads to excessive miss distances, while increasing the ratio beyond about 5 does not bring about a worthwhile decrease in miss distance in relation to the increased weight and cost of the missile.

9.4. The r.m.s. miss distance is practically constant over the range $a^2 = 0\cdot2$ to $0\cdot5$, so that this parameter can be chosen independently. It is preferable that a given r.m.s. miss distance should consist mostly of a steady bias with only a small dispersion, since this condition gives the least induced drag and reduces the demands on the control-surface actuators and oil supplies. These considerations point to a value of the missile acceleration lag in the neighbourhood of $0\cdot5$.

9.5. The analysis is restricted to target courses giving rise to a constant angular acceleration of the beam and a constant linear acceleration of the missile. No target fulfils these conditions, but they approximate with varying accuracy to a number of possible target trajectories at long range. It was shown in Section 5.2 that, for targets subject to the further restriction that $R_T\ddot{\theta} \gg 2\dot{R}_M\dot{\theta}$, the optimum value of the tracker lag A^2 is independent of $R_T\ddot{\theta}$—that is, of the target acceleration perpendicular to the beam. This however is not the case for other targets: if for example the target describes a circle around the tracker at constant velocity, the optimum tracker lag is infinite {equation (31)}, since $\ddot{\theta} = 0$. Practically this means that the tracker lag can be made very large without producing any beam lag; the consequent reduction in bandwidth reduces the beam jitter and hence the missile lag and dispersion.

For targets which do not conform to the above conditions, the damping factors δ (for the tracker) and u_C (for the missile) will have a considerable influence. For a moderately damped system the steady state is approached more quickly, but the miss distance is increased due to jitter; while a lightly damped system reduces the miss distance for 'steady-state targets' but also reduces the chance of reaching a steady state.

It is evident therefore that a more detailed study of target courses is required, weighted according to their frequency of occurrence and to the desirability of destruction. The system can then be re-assessed in the light of this information: it may then be desirable to vary the tracker parameters—particularly the acceleration lag—according to the type of engagement.

Acknowledgements.

The author is indebted to Mr. G. A. Whitfield, Mr. C. A. A. Wass, and Mr. R. G. Keats, for their helpful criticism and suggestions.

LIST OF SYMBOLS

A^2	Steady-state angular acceleration lag of tracker		sec^2
a^2	Steady-state linear acceleration lag of the missile		sec^2
D	Mean miss distance		ft
D_{min}	Minimum mean miss distance	for two dimensions	ft
D_{rms}	R.M.S. miss distance		ft
D', etc.	Miss distances for three dimensions		ft
G_T	Spectral Density of primary radar jitter		ft^2 sec
G_B	Spectral Density of beam jitter		ft^2 sec
$G\epsilon$	Spectral Density at input to missile control system		ft^2 sec
G	Spectral Density at output of phase-advance network		ft^2 sec
G'	Spectral Density at output of the limiter, i.e. the demanded acceleration		$ft^2\ sec^{-3}$
G_M	Spectral Density of the missile jitter		$ft^2\ sec^{-3}$
g_T	Target acceleration perpendicular to beam		ft sec^{-2}
g_M	Missile acceleration perpendicular to beam		ft sec^{-2}
g_S	Maximum permissible lateral acceleration of the missile		ft sec^{-2}
h_T	Instantaneous displacement of target		ft
h_B	Instantaneous displacement of beam	from a space datum	ft
h_M	Instantaneous displacement of missile		ft
$\langle h_T \rangle$, etc.	Mean displacement of target, etc., from a space datum		ft
J_T	Angular spectral density of radar jitter		sec
K	A constant of the tracker		
n	A constant of the phase-advance network		
R_T	Range of target from tracker		ft
R_M	Range of missile from tracker		ft
S	Stiffness of missile control loop		sec^{-2}
u_C	Damping ratio of the missile control weave		
u_W	Damping ratio of the missile weathercock mode		

LIST OF SYMBOLS—*continued*

$X(p)$	Transfer function of the phase-advance network	
$Y(p)$	Transfer function of the missile relating control-surface deflection to lateral displacement	
$Z(p)$	Transfer function of the tracker, relating the target angle to the beam angle	
δ	Damping ratio of tracker	
ϵ	Mean lag of missile behind beam	ft
ζ	Control-surface deflection expressed in units of demanded lateral acceleration	ft $\sec^{-2}$
θ	Sight-line angle from tracker to target	rad
σ_T^2	Variance of radar jitter	ft
σ_B^2	Variance of beam jitter	ft
σ^2	Variance at output of phase-advance network	ft
σ'^2	Variance at output of limiter, i.e. the variance of the demanded acceleration	ft $\sec^{-2}$
τ	Time constant of the phase-advance network	sec
ω_C	Frequency of missile control weave	rad. $\sec^{-1}$
ω_W	Frequency of missile weathercock mode	rad. $\sec^{-1}$
$\Delta\omega_T$	Noise bandwidth of the tracker	rad. $\sec^{-1}$
$\Delta\omega$	Noise bandwidth of the combination of tracker and phase-advance network	rad. $\sec^{-1}$

REFERENCE

No.	*Author*	*Title, etc*
1.	S. O. Rice	Mathematical analysis of random noise. *Bell System Tech. Journal*, Vol. XXIII. July, 1944, and Vol. XXIV January, 1945.

APPENDIX I

The Effect of Limits on a Combination of Signal and Noise

The input to the limiting device consists of a steady bias $\bar{x}$ representing the true error signal, together with random fluctuations having a mean value of zero and an amplitude distribution $\varphi(y)$. The distribution of the combination is then $\varphi(y-\bar{x})$.

The limiter is assumed to be such that

$$\begin{aligned} V' &= V, & -L < V < L, \\ V' &= L, & V \geqslant L, \\ V' &= -L, & -L \geqslant V, \end{aligned}$$

where the input is V and the output V'.

The proportion of amplitudes lying between the limits is

$$\int_{-L}^{L} \varphi(y-\bar{x})dy,$$

so that the contribution to the mean of these amplitudes is

$$\int_{-L}^{L} y\varphi(y-\bar{x})dy.$$

The probability that V exceeds L is

$$\int_{L}^{\infty} \varphi(y-\bar{x})dy,$$

and all of these amplitudes have the value L after limiting. Their contribution to the mean is therefore

$$L\int_{L}^{\infty} \varphi(y-\bar{x})dy.$$

Similarly, the amplitudes which are less than $-L$ give

$$-L\int_{-\infty}^{-L} \varphi(y-\bar{x})dy.$$

The mean output is therefore

$$\begin{aligned} \langle y \rangle &= \int_{-L}^{L} y\varphi(y-\bar{x})dy + L\int_{L}^{\infty} \varphi(y-\bar{x})dy - L\int_{-\infty}^{-L} \varphi(y-\bar{x})dy \\ &= \int_{-(L+\bar{x})}^{L-\bar{x}} (x+\bar{x})\varphi(x)dx + L\int_{L-\bar{x}}^{\infty} \varphi(x)dx - L\int_{-\infty}^{-(L+\bar{x})} \varphi(x)dx. \end{aligned}$$

An exactly similar argument gives the mean square output

$$\langle y^2 \rangle = \int_{-(L+\bar{x})}^{L-\bar{x}} (x+\bar{x})^2\varphi(x)dx + L^2\int_{L-\bar{x}}^{\infty} \varphi(x)dx + L^2\int_{-\infty}^{-(L+\bar{x})} \varphi(x)dx.$$

For a gaussian distribution,

$$\varphi(x) = \frac{1}{C\sqrt{\pi}} \exp\left(-\frac{x^2}{C^2}\right),$$

where $1/C$ is the modulus of precision. Substitution of this value in the above equations gives

$$\langle y \rangle = \tfrac{1}{2}(\bar{x}+L) \operatorname{erf}\left(\frac{\bar{x}+L}{C}\right) - \tfrac{1}{2}(\bar{x}-L) \operatorname{erf}\frac{\bar{x}-L}{C} - \frac{C}{\sqrt{\pi}} \exp\left(-\frac{\bar{x}^2+L^2}{C^2}\right) \sinh\frac{2\bar{x}L}{C^2}$$

and

$$\langle y^2 \rangle = L^2 + \tfrac{1}{2}\left(\frac{C^2}{2} + \bar{x}^2 - L^2\right)\left[\operatorname{erf}\left(\frac{\bar{x}+L}{C}\right) - \operatorname{erf}\left(\frac{\bar{x}-L}{C}\right)\right] -$$

$$- \frac{C}{\sqrt{\pi}} \exp\left(-\frac{\bar{x}^2+L^2}{C^2}\right)\left[L \cosh\frac{2\bar{x}L}{C^2} + \bar{x} \sinh\frac{2\bar{x}L}{C^2}\right].$$

APPENDIX II

The Spectral Density of a Stationary Random Process after a Non-Linear Device

1. In studying the effect of noise on the performance of a servo-mechanism or similar system, one is usually interested in the mean square value (and possibly other moments) at various points in the network—notably at the output. In a linear system this is completely specified by a knowledge of the spectral density of the noise at any one point, without reference to its amplitude distribution. Thus, if at the input to a network having the transfer function $F(p)$ the spectral density is G_{in}, the output spectral density is given by

$$G_{\text{out}} = |F(j\omega)|^2 G_{\text{in}},$$

and the mean square value of the output is

$$\sigma^2 = \int_0^\infty |F(j\omega)|^2 G_{\text{in}}\, d\omega .$$

For a non-linear device (such as a rectifier or limiter) which is insensitive to frequency, a knowledge of the amplitude distribution is sufficient to define the statistical properties of the output, as shown in Appendix I. The frequency distribution is in this case irrelevant, although it will of course be modified by the non-linear circuit.

The case in which the non-linear device forms part of an otherwise linear but frequency-sensitive system, is more complicated. This situation arises in the case of the beam rider, where the limits are followed by the missile transfer function $Y(p)$, and we are interested in the mean square value after $Y(p)$. This can only be obtained if the spectral density after limiting is known—the mean square value after limiting is by itself insufficient since $Y(p)$ is frequency sensitive. On the other hand, the spectral density after a non-linear device is not uniquely determined by the input spectral density alone—its amplitude distribution must also be specified.

2. Given these properties of the input—its spectral density and amplitude probability density—it is possible to deduce the spectral density after the non-linearity. In the analysis it is more convenient to deal with the correlation function rather than the spectral density. The former is defined as

$$R(\tau) = \operatorname*{Lim}_{T\to\infty} \frac{1}{2T} \int_{-T}^{T} V(t)V(t+\tau)dt,$$

where $V(t)$, $V(t+\tau)$ are the instantaneous values of the inputs at times t and $t+\tau$ respectively. The correlation function and the spectral density are intimately related—in fact they are Fourier Transforms of each other:

$$R(\tau) = \int_0^\infty G(\omega) \cos \omega\tau \, d\omega$$

and

$$G(\omega) = \frac{2}{\pi}\int_0^\infty R(\tau) \cos \omega\tau \, d\omega .$$

3. There are two methods for finding $R'(\tau)$, the output correlation function. The first, due to Van Vleck and North[1] is to integrate the bivariate probability density of $V(t)$ and $V(t+\tau)$ over

the domains allowed by the non-linear device. $V(t)$ and $V(t+\tau)$ can be considered as two random but correlated variables, and if the distribution of each is gaussian the joint probability density is

$$P\{V(t),\, V(t+\tau)\} = P(x_1, x_2)$$
$$= \frac{(\mu_{11}\mu_{22} - \mu_{12}^2)^{-1/2}}{2\pi} \exp\left[\frac{-\mu_{22}x_1^2 - \mu_{11}x_2^2 + 2\mu_{12}x_1x_2}{2(\mu_{11}\mu_{22} - \mu_{12}^2)}\right],$$

where x_1, x_2 have been written for $V(t)$, $V(t+\tau)$ respectively.

μ_{11}, μ_{22} are the second moments of the x_1's and the x_2's, while μ_{12} is a measure of the correlation between them.

Thus

$$\mu_{11} = \langle x_1^2 \rangle = \langle V(t)^2 \rangle = \sigma^2 = R(0)$$
$$\mu_{22} = \langle x_2^2 \rangle = \langle V(t+\tau)^2 \rangle = \sigma^2 = R(0)$$

and

$$\mu_{12} = \langle x_1 x_2 \rangle = \langle V(t)V(t+\tau) \rangle = R(\tau)$$

Inserting these values

$$P\{V(t),\, V(t+\tau)\} = P(x_1, x_2)$$
$$= \frac{(R(0)^2 - R(\tau)^2)^{-1/2}}{2\pi} \exp\left[\frac{-R(0)\,(x_1^2 + x_2^2) + 2R(\tau)x_1x_2}{2(R(0)^2 - R(\tau)^2)}\right] \tag{II.1}$$

We wish to find $R'(\tau)$, the correlation function after the non-linear device. This is the average value of $x_1'x_2'$, where x_1', x_2' are instantaneous output amplitudes corresponding to the inputs x_1, x_2. The product $x_1'x_2'$ is clearly a function of x_1 and x_2:

$$x_1'x_2' = f(x_1, x_2),$$

where the nature of the function is determined by the non-linear device.

The average value of any function $f(x_1, x_2)$ is, from (II.1)

$$\int_{-\infty}^{\infty} dx_1 \int_{-\infty}^{\infty} dx_2 f(x_1, x_2) P(x_1, x_2),$$

so that

$$R'(\tau) = \int_{-\infty}^{\infty} dx_1 \int_{-\infty}^{\infty} dx_2 f(x_1, x_2) \frac{(R(0)^2 - R(\tau)^2)^{-1/2}}{2\pi} \times$$
$$\times \exp\left[\frac{-R(0)\,(x_1^2 + x_2^2) + 2R(\tau)x_1x_2}{2(R(0)^2 - R(\tau)^2)}\right]. \tag{II.2}$$

The spectral density at the output is then given by

$$G'(\omega) = \frac{2}{\pi}\int_0^{\infty} R'(\tau) \cos \omega\tau \, d\tau. \tag{II.3}$$

4. *The Linear Rectifier.*

4.1. The function $f(x_1, x_2)$ will in general be different for different ranges of x_1 and x_2. A simple example is a linear rectifier, which is such that

$$V' = \begin{cases} V, & V > 0 \\ 0, & V \leqslant 0 \end{cases}$$

(V, V' are instantaneous values of input and output respectively).

In this case therefore

$$x_1'x_2' = f(x_1, x_2) = \begin{cases} x_1x_2, \; x_1 > 0, \; x_2 > 0 \\ 0 \quad \text{elsewhere,} \end{cases}$$

so that from (II.2)

$$R'(\tau) = \int_0^\infty dx_1 \int_0^\infty dx_2 x_1 x_2 \frac{(R(0)^2 - R(\tau)^2)^{-1/2}}{2\pi} \times$$
$$\times \exp\left[\frac{-R(0)\,(x_1^2+x_2^2) + 2R(\tau)x_1x_2}{2(R(0)^2 - R(\tau)^2)}\right].$$

This reduces to

$$R'(\tau) = \frac{R(0)}{2\pi}\left[\rho\left\{\frac{\pi}{2} + \tan^{-1}\left(\frac{\rho}{\sqrt{(1-\rho^2)}}\right)\right\} + \sqrt{(1-\rho^2)}\right], \qquad \text{(II.4)}$$

where $\rho = R(\tau)/R(0)$, the normalised autocorrelation function of the input.

4.2. *Input Spectral Density Constant with Frequency.*

If the spectral density at the input to the linear rectifier is constant with frequency, the input autocorrelation function is a delta function at $\tau = 0$.

Thus

$$\begin{aligned} \rho &= 1, \qquad \tau = 0 \\ &= 0, \qquad \tau \neq 0, \end{aligned}$$

so that, from (II.4)

$$\begin{aligned} R'(\tau) &= \frac{R(0)}{2} = \frac{\sigma^2}{2}, \qquad \tau = 0 \\ &= \frac{R(0)}{2\pi} = \frac{\sigma^2}{2\pi}, \qquad \tau \neq 0 \end{aligned}$$

where σ^2 is the variance at the input.

The constant term $\sigma^2/2\pi$ represents the d.c. term of magnitude $\sigma/\sqrt{(2\pi)}$ produced by rectification of the noise: it will appear as a delta function at $\omega = 0$ in the output spectral density. The term $R(0)/2$ at $\tau = 0$ gives a spectral density that is constant with frequency.

Thus the linear rectifier does not alter the shape of the spectral density if the input is 'white noise'. The r.m.s. output is $\sigma/\sqrt{2}$, and a d.c. term of magnitude $\sigma/\sqrt{(2\pi)}$ is produced.

4.3. *Input Spectral Density Constant up to Cut-off Frequency.*

If the input power spectrum is constant up to frequency ω_0, and zero thereafter, then

$$R(\tau) = \int_0^{\omega_0} k^2 \cos\omega\tau \, d\omega = \frac{k^2}{\tau}\sin\omega_0\tau,$$

where

$$\begin{aligned} G(\omega) &= k^2, \qquad \omega < \omega_0 \\ &= 0, \qquad \omega > \omega_0. \end{aligned}$$

Thus

$$R(0) = k^2\omega_0,$$

and

$$\rho = \frac{R(\tau)}{R(0)} = \frac{\sin\omega_0\tau}{\omega_0\tau}.$$

Substituting this value for ρ in (II.4), and then using (II.3),

$$G'(\omega) = \frac{k^2\omega_0}{\pi^2}\int_0^\infty \left[\frac{\sin\omega_0\tau}{\omega_0\tau}\left\{\frac{\pi}{2} + \tan^{-1}\left(\frac{\sin\omega_0\tau/\omega_0\tau}{\sqrt{\{1-(\sin\omega_0\tau/\omega_0\tau)^2\}}}\right)\right\} + \right.$$

$$\left. + \sqrt{\left\{1 - \left(\frac{\sin\omega_0\tau}{\omega_0\tau}\right)^2\right\}}\right] \cos\omega\tau\, d\tau\,.$$

On putting

$$\omega_0\tau = x\,,$$

$$G'(\omega) = \frac{k^2}{\pi^2}\int_0^\infty \left[\frac{\sin x}{x}\left\{\frac{\pi}{2} + \tan^{-1}\left(\frac{\sin x/x}{\sqrt{\{1-(\sin x/x)^2\}}}\right)\right\} + \right.$$

$$\left. + \sqrt{\left\{1 - \left(\frac{\sin x}{x}\right)^2\right\}} - 1\right] \cos\frac{\omega}{\omega_0}x\, dx + \frac{k^2}{\pi^2}\int_0^\infty \cos\frac{\omega}{\omega_0}x\, dx\,. \qquad \text{(II.5)}$$

This expression for the output spectral density is plotted in Fig. 9, omitting the second integral, which represents the d.c. term. It will be seen that the action of the rectifier is to spread the spectrum in the neighbourhood of the cut-off frequency. The spread becomes less as ω_0 is increased: in the limiting case of $\omega_0 \to \infty$, the spectrum remains unchanged, as was shown in Section 4.2.

The output mean square value is $R'(0)$, and can be found by putting $\rho = 1$ (its value at $\tau = 0$) in equation (II.4)

$$R'(0) = \frac{R(0)}{2} = \frac{k^2\omega_0}{2} = \frac{\sigma^2}{2}\,,$$

so that the r.m.s. output is $\sigma/\sqrt{2}$.

The d.c. term is given by $\sqrt{\{R'(\infty)\}}$, since the autocorrelation of a constant K is K^2.

Thus

$$\lim_{\tau\to\infty} \rho = \lim_{\tau\to\infty} \frac{\sin\omega_0\tau}{\omega_0\tau} = 0\,,$$

and, from (II.4)

$$R'(\infty) = \frac{R(0)}{2\pi} = \frac{k^2\omega_0}{2\pi} = \frac{\sigma^2}{2\pi}\,,$$

so that the d.c. term is $\sigma/\sqrt{(2\pi)}$.

Alternatively, the d.c. term may be found from the output spectral density $G'(\omega)$, equation (II.5). The second integral of this equation is a delta singularity at $\omega = 0$, so that its area is the square of the d.c. term, given by

$$\int_0^\infty d\omega\, \frac{k^2}{\pi^2}\int_0^\infty \cos\frac{\omega}{\omega_0}x\, dx = \frac{k^2\omega_0}{2\pi} = \frac{\sigma^2}{2\pi}\,.$$

The d.c. term is therefore $\sigma/\sqrt{(2\pi)}$, as before.

The mean and r.m.s. outputs can of course be obtained directly from a consideration of the amplitude distribution of the input, as was shown in Appendix I for the case of the limiter. The input distribution is assumed to be gaussian, so that

$$\text{Mean Output} = \frac{1}{C\sqrt{\pi}}\int_0^\infty x\exp\left(-\frac{x^2}{C^2}\right)dx = \frac{C}{2\sqrt{\pi}} = \sigma/\sqrt{(2\pi)}\,,$$

and

$$\text{Mean Square Output} = \frac{1}{C\sqrt{\pi}}\int_0^\infty x^2\exp\left(-\frac{x^2}{C^2}\right)dx = C^2 = \frac{\sigma^2}{2}\,.$$

These values agree with those deduced above from the output autocorrelation function and spectral density.

5. *The Limiter.*

For the limiter, defined by

$$
\begin{aligned}
V' &= V \qquad && -L < V < L \\
&= L && V \geqslant L \\
&= -L, && V \leqslant -L,
\end{aligned}
$$

the required function is

$$
x_1'x_2' = f(x_1, x_2) = \begin{cases}
x_1x_2, & -L < x_1 < L, \quad -L < x_2 < L \\
Lx_2, & x_1 \geqslant L, \quad -L < x_2 < L \\
-Lx_2, & x_1 \leqslant -L, \quad -L < x_2 < L \\
Lx_1, & -L < x_1 < L, \quad x_2 \geqslant L \\
-Lx_1, & -L < x_1 < L, \quad x_2 \leqslant -L \\
L^2, & x_1 \geqslant L, \quad x_2 \geqslant L \\
L^2, & x_1 \leqslant -L, \quad x_2 \leqslant -L \\
-L^2, & x_1 \geqslant -L, \quad x_2 \leqslant -L \\
-L^2, & x_1 \leqslant -L, \quad x_2 \geqslant L.
\end{cases}
$$

Substitution for $f(x_1, x_2)$ in (II.2) gives $R'(\tau)$ as the sum of nine double integrals corresponding to the nine domains of $f(x_1, x_2)$:

$$
\begin{aligned}
R'(\tau) = & \int_{-L}^{L} dx_1 \int_{-L}^{L} dx_2 x_1 x_2 P + L \int_{L}^{\infty} dx_1 \int_{-L}^{L} dx_2 x_2 P - \\
& - L \int_{-\infty}^{-L} dx_1 \int_{-L}^{L} dx_2 x_2 P + L \int_{-L}^{L} dx_1 \int_{L}^{\infty} dx_2 x_1 P - L \int_{-L}^{L} dx_1 \int_{-\infty}^{-L} dx_2 x_1 P + \\
& + L^2 \int_{L}^{\infty} dx_1 \int_{L}^{\infty} dx_2 P + L^2 \int_{-\infty}^{-L} dx_1 \int_{-\infty}^{-L} dx_2 P - L^2 \int_{L}^{\infty} dx_1 \int_{-\infty}^{-L} dx_2 P - \\
& - L^2 \int_{-\infty}^{-L} dx_1 \int_{L}^{\infty} dx_2 P,
\end{aligned}
$$

where

$$
P = \frac{\{R(0)^2 - R(\tau)^2\}^{-1/2}}{2\pi} \exp\left[\frac{-R(0)\,(x_1^2 + x_2^2) + 2R(\tau)x_1x_2}{2\{R(0)^2 - R(\tau)^2\}}\right].
$$

This gives a definite expression for $R'(\tau)$ in terms of $R(\tau)$, $R(0)$ and L, and the output spectral density is then given by (II.3). The expression is obviously too complex to use in the analysis of the beam rider, but it is possible to estimate the error involved in the assumption of Section 3.2 of the main text for a given case.

6. The second method uses the fact that a number of non-linear devices can be described as a contour integral of the form

$$V' = \frac{1}{2\pi} \int_C f(iu) e^{iVu} du ,$$

where the contour is chosen to fit the device. This avoids integrating over a number of domains, as is necessary in the above method, but the particular case of the limiter again leads to integrals which are difficult to evaluate.

7. The results of Section 4 show that for the particular case of white noise with a given cut-off frequency, the spectral density is not greatly altered by a linear rectifier (Fig. 9). It is reasonable to suppose that this conclusion is also valid for the limiter, since the latter introduces a more symmetrical and less severe form of distortion. The difference between input and output spectral densities will be most marked at the higher frequencies, but the filtering action of the missile will tend to reduce the error introduced by assuming that the spectral densities before and after limiting are in fact identical.

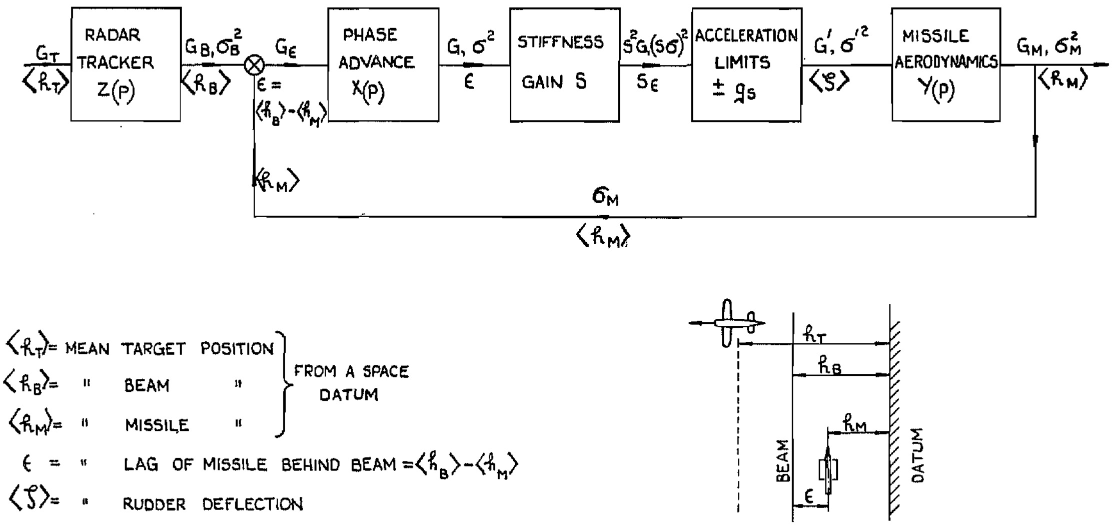

FIG 1. Schematic diagram of beam-riding system.

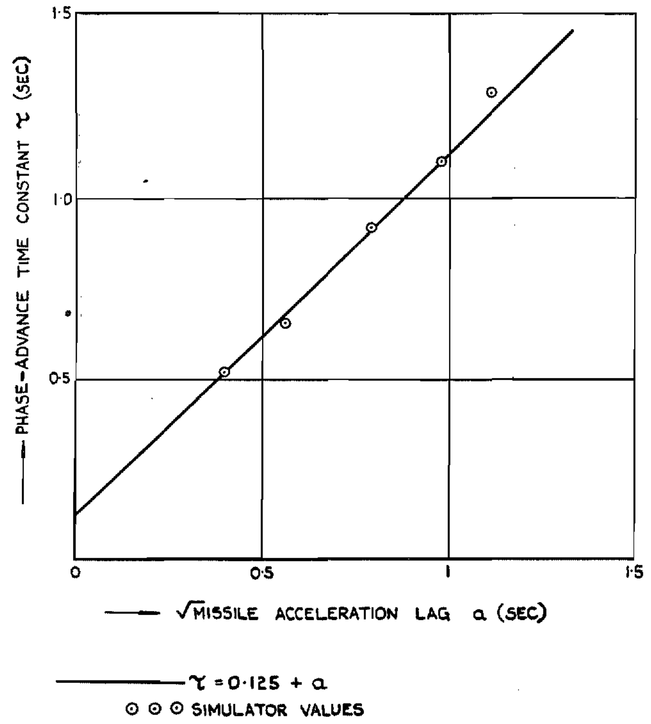

FIG 2. Relation between phase-advance time constant and missile acceleration lag.

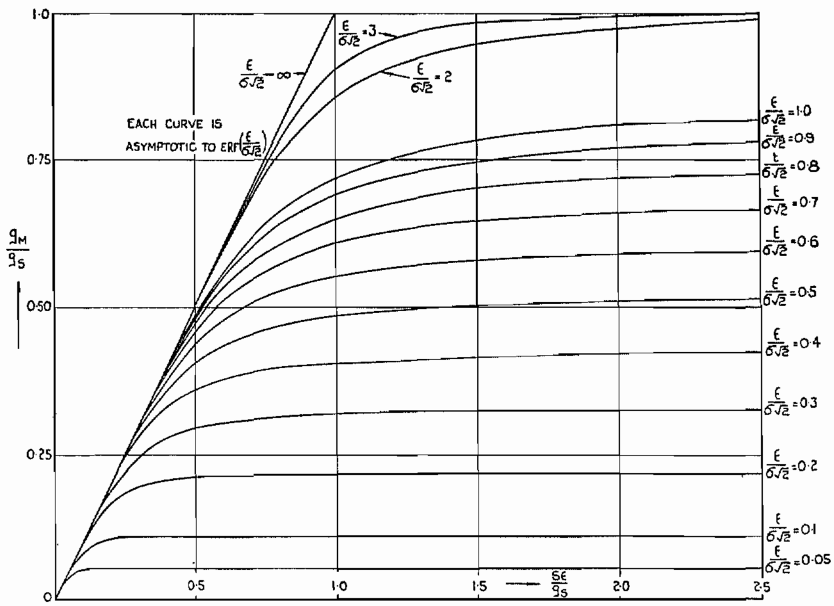

FIG 3. Graph showing influence of jitter and limits on mean output of limiter {Equation (11)}.

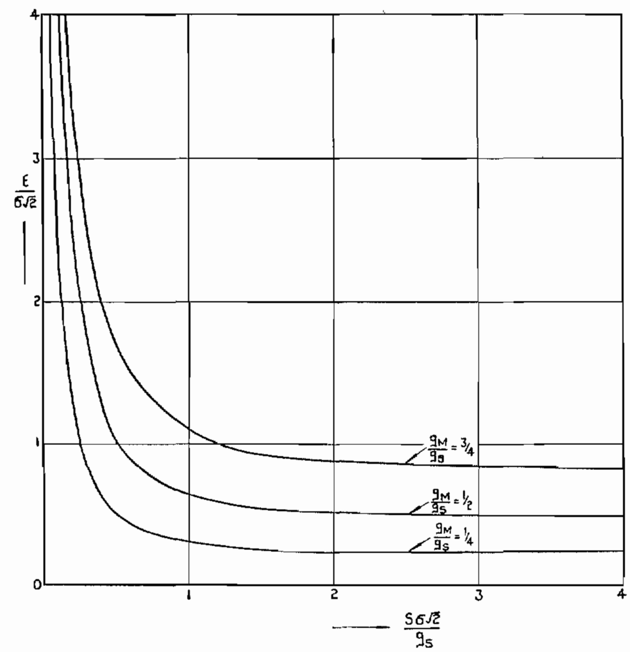

FIG. 4. Graph of $\epsilon/\sigma\sqrt{2}$ vs. $S\sigma\sqrt{2}/g_S$ {Equation (11)}.

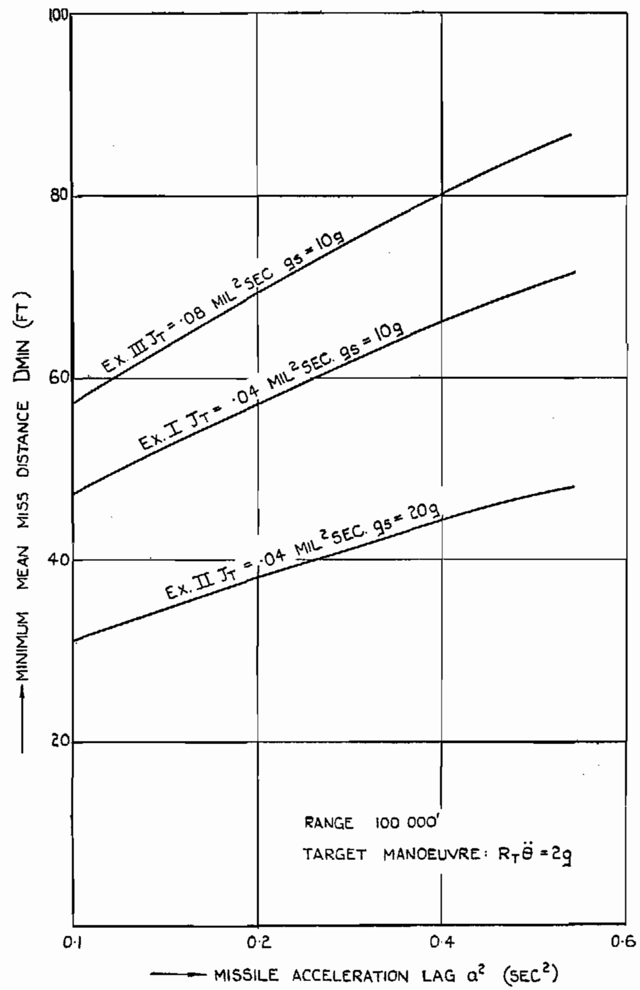

FIG. 5. Variation of minimum mean miss distance with missile acceleration lag.

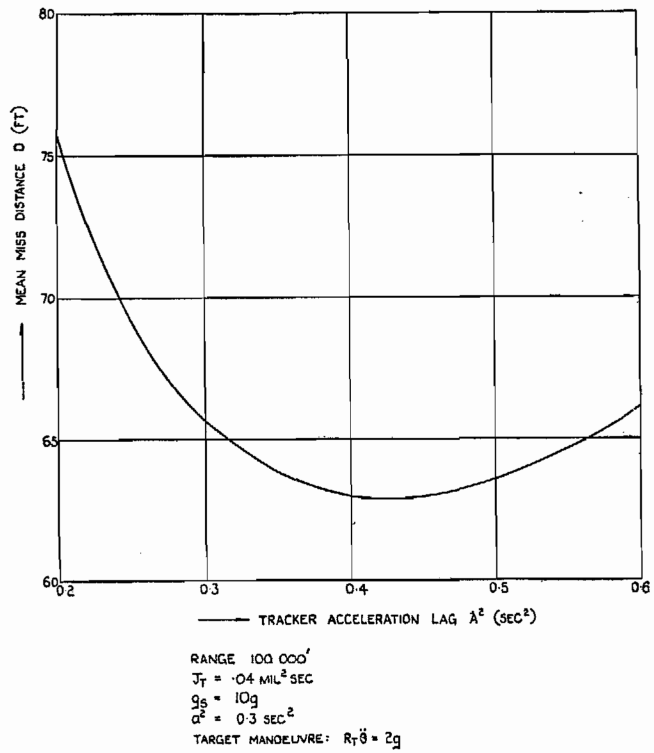

FIG. 6. Variation of mean miss distance with tracker acceleration lag.

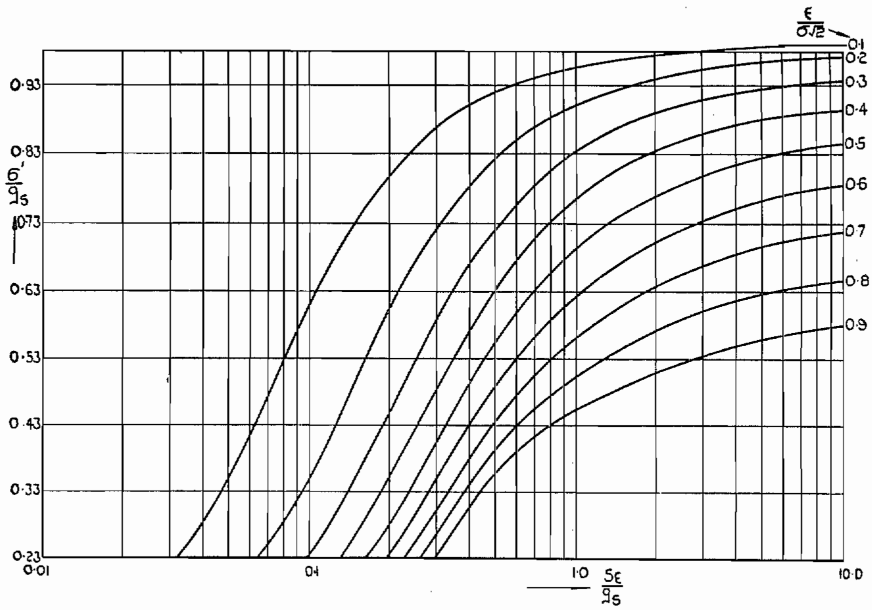

FIG. 7. Variance at limiter output {Equation (12)}.

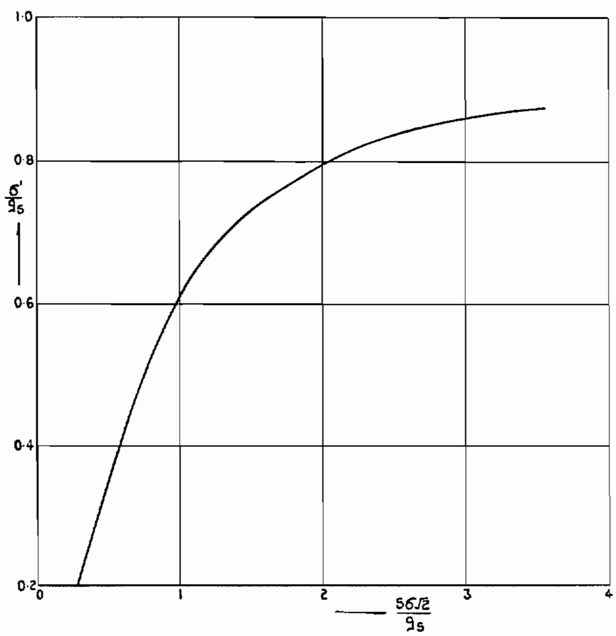

FIG. 8. Graph of σ'/g_S vs. $S\sigma\sqrt{2}/g_S$.

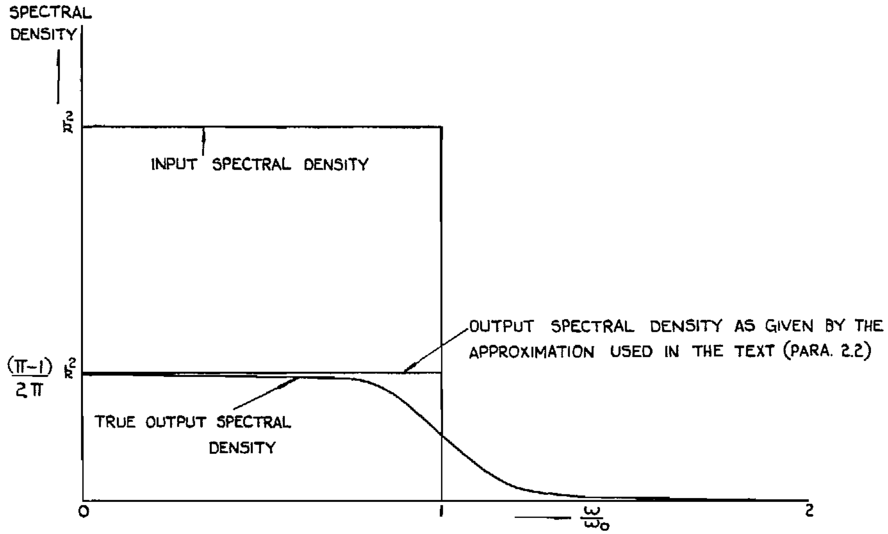

FIG. 9. The effect on spectral density of a linear rectifier.

(92139) Wt.67 K5 3/66 Hw.

Publications of the Aeronautical Research Council

ANNUAL TECHNICAL REPORTS OF THE AERONAUTICAL RESEARCH COUNCIL (BOUND VOLUMES)

1945 Vol. I. Aero and Hydrodynamics, Aerofoils. £6 10*s*. (£6 13*s*. 6*d*.)
Vol. II. Aircraft, Airscrews, Controls. £6 10*s*. (£6 13*s*. 6*d*.)
Vol. III. Flutter and Vibration, Instruments, Miscellaneous, Parachutes, Plates and Panels, Propulsion. £6 10*s*. (£6 13*s*. 6*d*.)
Vol. IV. Stability, Structures, Wind Tunnels, Wind Tunnel Technique. £6 10*s*. (£6 13*s*. 3*d*.)

1946 Vol. I. Accidents, Aerodynamics, Aerofoils and Hydrofoils. £8 8*s*. (£8 11*s*. 9*d*.)
Vol. II. Airscrews, Cabin Cooling, Chemical Hazards, Controls, Flames, Flutter, Helicopters, Instruments and Instrumentation, Interference, Jets, Miscellaneous, Parachutes. £8 8*s*. (£8 11*s*. 3*d*.)
Vol. III. Performance, Propulsion, Seaplanes, Stability, Structures, Wind Tunnels. £8 8*s*. (£8 11*s*. 6*d*.)

1947 Vol. I. Aerodynamics, Aerofoils, Aircraft. £8 8*s*. (£8 11*s*. 9*d*.)
Vol. II. Airscrews and Rotors, Controls, Flutter, Materials, Miscellaneous, Parachutes, Propulsion, Seaplanes, Stability, Structures, Take-off and Landing. £8 8*s*. (£8 11*s*. 9*d*.)

1948 Vol. I. Aerodynamics, Aerofoils, Aircraft, Airscrews, Controls, Flutter and Vibration, Helicopters, Instruments, Propulsion, Seaplane, Stability, Structures, Wind Tunnels. £6 10*s*. (£6 13*s*. 3*d*.)
Vol. II. Aerodynamics, Aerofoils, Aircraft, Airscrews, Controls, Flutter and Vibration, Helicopters, Instruments, Propulsion, Seaplane, Stability, Structures, Wind Tunnels. £5 10*s*. (£5 13*s*. 3*d*.)

1949 Vol. I. Aerodynamics, Aerofoils. £5 10*s*. (£5 13*s*. 3*d*.)
Vol. II. Aircraft, Controls, Flutter and Vibration, Helicopters, Instruments, Materials, Seaplanes, Structures, Wind Tunnels. £5 10*s*. (£5 13*s*.)

1950 Vol. I. Aerodynamics, Aerofoils, Aircraft. £5 12*s*. 6*d*. (£5 16*s*.)
Vol. II. Apparatus, Flutter and Vibration, Meteorology, Panels, Performance, Rotorcraft, Seaplanes. £4 (£4 3*s*.)
Vol. III. Stability and Control, Structures, Thermodynamics, Visual Aids, Wind Tunnels. £4 (£4 2*s*. 9*d*.)

1951 Vol. I. Aerodynamics, Aerofoils. £6 10*s*. (£6 13*s*. 3*d*.)
Vol. II. Compressors and Turbines, Flutter, Instruments, Mathematics, Ropes, Rotorcraft, Stability and Control, Structures, Wind Tunnels. £5 10*s*. (£5 13*s*. 3*d*.)

1952 Vol. I. Aerodynamics, Aerofoils. £8 8*s*. (£8 11*s*. 3*d*.)
Vol. II. Aircraft, Bodies, Compressors, Controls, Equipment, Flutter and Oscillation, Rotorcraft, Seaplanes, Structures. £5 10*s*. (£5 13*s*.)

1953 Vol. I. Aerodynamics, Aerofoils and Wings, Aircraft, Compressors and Turbines, Controls. £6 (£6 3*s*. 3*d*.)
Vol. II. Flutter and Oscillation, Gusts, Helicopters, Performance, Seaplanes, Stability, Structures, Thermodynamics, Turbulence. £5 5*s*. (£5 8*s*. 3*d*.)

1954 Aero and Hydrodynamics, Aerofoils, Arrester gear, Compressors and Turbines, Flutter, Materials, Performance, Rotorcraft, Stability and Control, Structures. £7 7*s*. (£7 10*s*. 6*d*.)

Special Volumes

Vol. I. Aero and Hydrodynamics, Aerofoils, Controls, Flutter, Kites, Parachutes, Performance, Propulsion, Stability. £6 6*s*. (£6 9*s*.)
Vol. II. Aero and Hydrodynamics, Aerofoils, Airscrews, Controls, Flutter, Materials, Miscellaneous, Parachutes, Propulsion, Stability, Structures. £7 7*s*. (£7 10*s*.)
Vol. III. Aero and Hydrodynamics, Aerofoils, Airscrews, Controls, Flutter, Kites, Miscellaneous, Parachutes, Propulsion, Seaplanes, Stability, Structures, Test Equipment. £9 9*s*. (£9 12*s*. 9*d*.)

Reviews of the Aeronautical Research Council

1949–54 5*s*. (5*s*. 5*d*.)

Index to all Reports and Memoranda published in the Annual Technical Reports

1909–1947 R. & M. 2600 (out of print)

Indexes to the Reports and Memoranda of the Aeronautical Research Council

Between Nos. 2451–2549: R. & M. No. 2550 2*s*. 6*d*. (2*s*. 9*d*.); Between Nos. 2651–2749: R. & M. No. 2750 2*s*. 6*d*. (2*s*. 9*d*.); Between Nos. 2751–2849: R. & M. No. 2850 2*s*. 6*d*. (2*s*. 9*d*.); Between Nos. 2851–2949: R. & M. No. 2950 3*s*. (3*s*. 3*d*.); Between Nos. 2951–3049: R. & M. No. 3050 3*s*. 6*d*. (3*s*. 9*d*.); Between Nos. 3051–3149: R. & M. No. 3150 3*s*. 6*d*. (3*s*. 9*d*.); Between Nos. 3151–3249: R. & M. No. 3250 3*s*. 6*d*. (3*s*. 9*d*.); Between Nos. 3251–3349: R. & M. No. 3350 3*s*. 6*d*. (3*s*. 10*d*.)

Prices in brackets include postage

Government publications can be purchased over the counter or by post from the Government Bookshops in London, Edinburgh, Cardiff, Belfast, Manchester, Birmingham and Bristol, or through any bookseller

R. & M. No. 3417

Printed and published by
HER MAJESTY'S STATIONERY OFFICE

To be purchased from
49 High Holborn, London WC1
423 Oxford Street, London W1
13A Castle Street, Edinburgh 2
109 St. Mary Street, Cardiff
Brazennose Street, Manchester 2
50 Fairfax Street, Bristol 1
35 Smallbrook, Ringway, Birmingham 5
80 Chichester Street, Belfast 1
or through any bookseller

Printed in England

R. & M. No. 3417

S.O. Code No. 23-3417